CHARACTERIZATION OF THE RESERVOIR POTENTIAL OF THE H-T FIELD, WALVIS BASIN, OFFSHORE NAMIBIA

A THESIS SUBMITTED IN PARTIAL FULFILMENT OF THE

REQUIREMENTS FOR THE DEGREE

OF

MASTER OF SCIENCE IN PETROLEUM GEOSCIENCES

OF

THE UNIVERSITY OF NAMIBIA

BY

JOEL NDANGI IYAMBO

200212125

OCTOBER 2024

MAIN SUPERVISOR: Dr. Collen-Issia Uahengo (University of Namibia)

CO-SUPERVISOR: Professor Mimonitu Opuwari (University of the Western Cape)

ABSTRACT

The Walvis Basin, renowned for its hydrocarbon potential, has long attracted the attention of the oil and gas industry. However, effective reservoir characterization remains a critical challenge, influencing exploration and development strategies. This study addresses the need for detailed reservoir characterization and its role in enhancing hydrocarbon prospectivity in the H-T field of the Walvis Basin. The impetus motivating this research is the lack of comprehensive reservoir characterization, leading to uncertainties in the distribution of hydrocarbon-bearing zones and their petrophysical properties. A study of reservoir characterization using well logs has been conducted to address the above-mentioned problem. Four wells in the H-T field were selected for analysis, and an array of well logs, including gamma ray, resistivity, neutron, and density logs, was employed to evaluate the petrophysical properties of identified reservoir rocks. The Interactive Petrophysics software facilitated the systematic evaluation of these properties. The gamma ray log was harnessed for lithologic discrimination, enabling the identification of discrete reservoir formations. The resistivity log played a pivotal role in determining the nature of formation fluids based on the electrical responses of reservoir formations. Furthermore, the combined analysis of density and neutron logs was instrumental in estimating reservoir porosity and identifying the presence of hydrocarbons where applicable. The results of this study unveiled the presence of three water-bearing reservoirs in Well HT3 namely Y1, Y2 and Y3 with thicknesses of 55.47 m, 5.03 m, and 10.52 m, respectively. Additionally, reservoir correlation, facilitated by the gamma ray log, revealed a discontinuous distribution of reservoirs across the wells. Furthermore, a cross-plot analysis of water saturation and porosity unveiled variations in grain size, ranging from fine-grained to silty sands within the reservoirs. This research significantly contributes to the understanding of reservoir characteristics, their distribution, and hydrocarbon prospectivity in the H-T field of the Walvis Basin. It provides essential insights for future exploration and production endeavors, offering a more informed approach to hydrocarbon resource assessment and development in the region.

Keywords: Walvis Basin, Reservoir characterization, Well logs interpretation, hydrocarbon prospectivity

LIST OF COFERENCE PROCEEDINGS

Poster Presentation at the EAGE Sub-Saharan Africa Energy Forum 04-06 March 2024: Characterization of the reservoir potential of selected Wells in the Walvis Basin, Offshore Namibia – J. Ndangi Iyambo[1], C. Uahengo[1], M. Opuwari[2], A. Narubes[3], P. Sindimba[3]

[1]University of Namibia

[2]University of Western Cape

[3]NAMCOR

TABLE OF CONTENTS

LIST OF TABLES

LIST OF FIGURES

LIST OF ABREVIATIONS AND /OR ACRONYMS

API: American Petroleum Institute

CL: Caliper

GR: Gamma Ray

IP: Interactive Petrophysics

ILm: Medium Induction

K: Permeability

K_e: Effective Permeability

LLd: Deep Laterolog Device

LLs: Shallow Laterolog

Ma: Mega annum (one-million years ago)

M_d: Millidarcies

LAS: LASer File Format

MIS: Matrix Identification

NAMCOR: National Petroleum Corporation of Namibia

NPHI: Neutron Porosity

NTG: Net to Gross

PEE: Photoelectric Effect

PETROFUND: Petroleum Training and Education Fund

PHIE: Effective Porosity

PHIT: Total Porosity

RHOB: Bulk Density

SP: Spontaneous Potential

S_g: Gas Saturation

S_h: Hydrocarbon Saturation

S_o: Oil Saturation

S_w: Water Saturation

S_{wirr}: Irreducible Water Saturation

S_{xo}: Flushed Zone

TOC: Total Organic Content

$_U$D: Microdarcy

UNAM: University of Namibia

Vcl: Volume of Clay

V_{sh}: Volume of Shale

V/V: decimal ratio of volume

%: Percentage

ACKNOWLEGMENTS

I am indebted to many people who have played a significant role in assisting me during my MSc journey. I would like to express my sincere gratitude and appreciation to my supervisors, Dr Collen-Issia Uahengo and Prof Mimonitu Opuwari, for their support, guidance, and willingness to review my work and provide constructive feedback. It has been an incredibly rewarding experience working with you both, especially having to integrate your expertise for better insight into reservoir characterization.

Special thanks are due to the Petroleum Training and Education Fund (PETROFUND) for funding the research project and the National Petroleum Corporation of Namibia (NAMCOR) Ltd, for supplying data used in this study. I would like to acknowledge Geoactive Limited for providing IP software to the University of Namibia which was used for this study as well as the University of Namibia for providing Workstation for my research data processing and interpretation.

I would also like to extend my thanks to my two classmates (Justina Hamalwa and Ester David) for those lunchtime conversations. I appreciate you all for providing me with personal and professional guidance. I am grateful to my friends for their support and prayers.

Above all, I would like to thank my wife Katsheeta, Gwetu (son) and Ayishe (daughter) for the selfless love, support, and unremitting encouragement. Thank you, dear wife, for always being there to listen and support any decision I made although you hardly understood what my research was about. I would never be able to pay back the love and sacrifices you made to shape my life. I could not have been blessed with more amazing family.

DEDICATIONS

To my parents (Tate Atanasius Ntoni Festus na Meme Loide Tshuutheni Shaanika), wife (Katsheeta) and children (Gwetu na Ayishe). With love and thanks.

DECLARATION

I, Joel Ndangi Iyambo, hereby declare that this study is my own work and is a true reflection of my research, and that this work, or any part thereof has not been submitted for a degree at any other institution.

Joel Ndangi Iyambo	……	October 2024
Name of Student	**Signature**	**Date**

CHAPTER 1: INTRODUCTION

1.1 Background of the Study

The Namibian offshore has historically been overlooked as an oil province, but recent discoveries such as Venus, Graff, and Jonker-1X in the Orange Basin indicate its potential as a promising area for oil discoveries. The presence of effective reservoirs is seen as the main risk, influencing exploration and development strategies (McDermott et al., 2015; Chandler et al., 2018).

Petrophysical analysis of well logs is considered one of the most valuable and important tools for characterizing reservoir rocks (Senosy et al., 2020). This analysis helps define crucial physical properties of rocks including lithology, porosity, permeability, and fluid saturation (Lyaka & Mulino, 2018). Porosity and permeability are the two main microscopic scale rock properties that influence fluid storage and flow in a reservoir (Al-Jawad & Saleh, 2019). Roger (2006) collectively called porosity and permeability as “reservoir quality’.

Furthermore, the petrophysical analysis is also useful in delineating potential reservoir intervals (Afizu, 2013), distinguishing the type of fluid in a reservoir and estimating hydrocarbon reserves (Das & Chatterjee, 2018). This can be achieved by utilizing well logs data, such as gamma ray, density, neutron porosity log, photoelectric effect values, and resistivity logs.

The primary aim of this study was to interpret log data well and conduct a quantitative evaluation of petrophysical properties to identify zones with the potential for hydrocarbon accumulation based on variations in depth and thickness.

1.2 Exploration History

The offshore of Namibia is an underexplored area with only 23 wells drilled in an area of more than 500,000 square kilometers ("History, 2022"; Figure 1). Petroleum exploration offshore Namibia started in the Orange Basin in the late 1960s, culminating with the discovery in 1974, of a dry gas by the Kudu 9A-1 well, in Barremian eolian sandstones (Mello et al., 2012). A gas-prone paradigm was established and lasted for almost 54 years, stopping any exploration campaigns in the area, until the discovery, in 2012, of a 41º API, marine siliciclastic oil, source by the Aptian/ Barremian marine anoxic, in the Wingat-1 well in the Walvis Basin (Mello et al, 2013).

Walvis Basin has only attracted significant interest after Namibia gained political independence from South Africa in 1990. Despite the existence of extensive 2D and 3D seismic data coverage of the Walvis Basin, the basin remains largely under explored with only eight exploration wells drilled to date in this basin. The first exploration well (1911/15-1) was completed in early 1994 by Norsk Hydro (Holter and Forsberg, 2000).

Wingat and Murombe wells were drilled in 2012, proving the presence of excellent to

good quality, mature, marine, oil-prone Aptian source rock (Galp Energia, 2013). Light oil, although not in commercial volumes, was recovered from a thin sandstone within the Aptian to Albian aged source rock interval in the Wingat-1 (Mello et al., 2013; Galp Energia, 2013).

Following the derisking of source rock presence, a 1,000 km of 2D seismic and 3,440 km^2 3D seismic data were acquired across the Walvis Basin (McDermott et al., 2015). A new prospect was identified and tested by drilling the Cormorant well in 2017. This well penetrated and assessed the hydrocarbon potential of a Cenomanian-aged base-of-slope turbidite fan primary target. The Cormorant Fan sandstones encountered in the primary objective of the well proved to be water bearing (Brink, 2018).

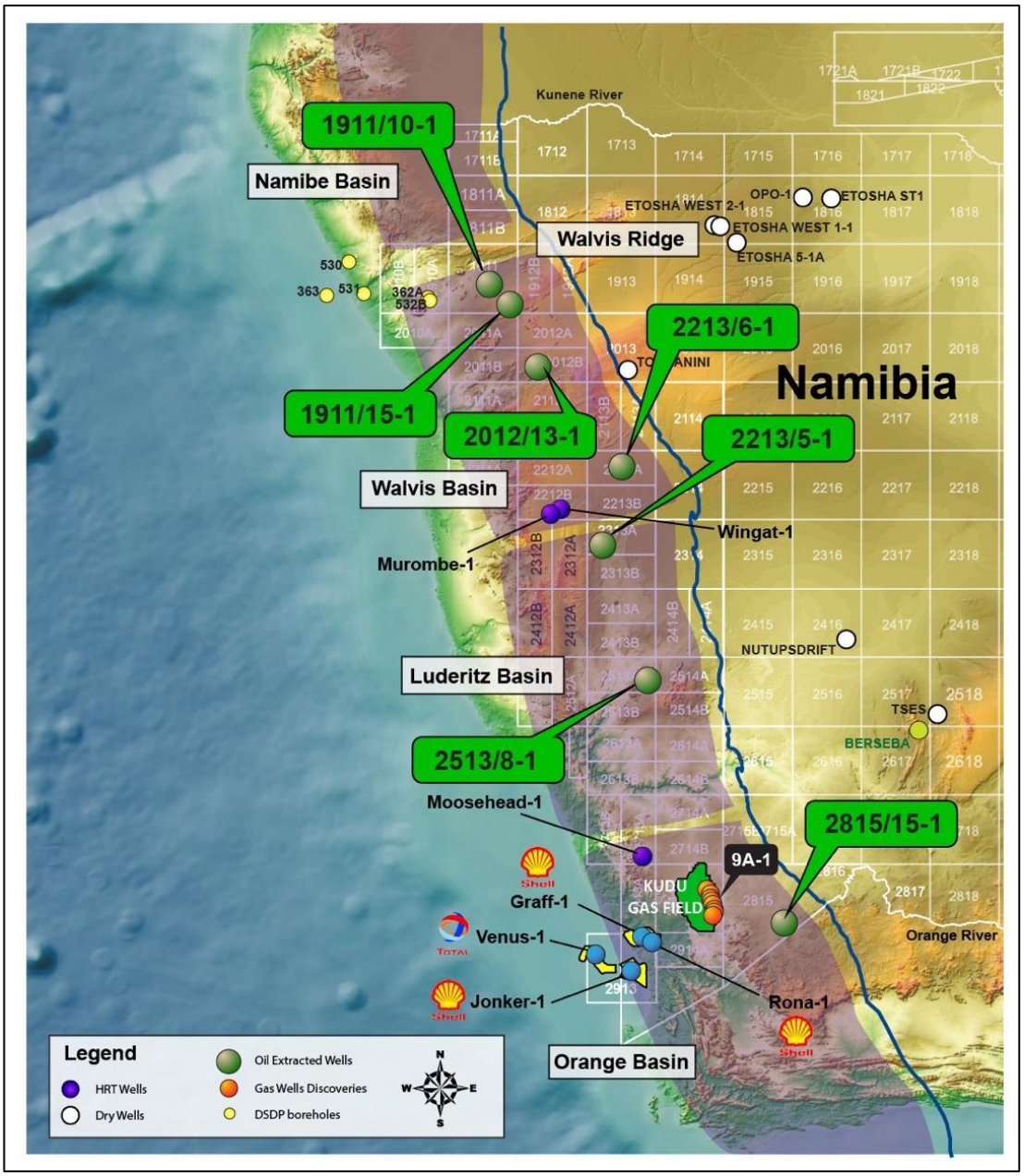

Figure 1: Map of offshore Namibia showing wells drilled up to end of 2022 (Adopted from Mello, 2022).

Overall, the exploratory wells within the Walvis Basin have intersected structural closures and channel sandstones within the Upper Cretaceous but have failed to locate significant hydrocarbon accumulations (Mello, 2022). A possible reason for failure

may be the lack of vertical migration from the mature Aptian source to the shallower and apparently more sand-prone sequences (Brink, 2018).

Kukulus (2004) conducted a study involving a 2D section through the central part of the Walvis Basin. This study integrated an assessment of hydrocarbon potential utilizing all available data from shallow water drilling and seismic surveys. The examination of potential reservoir intervals developed in the central and northern Walvis Basin revealed three potential reservoir rock intervals developed in the early to late drift succession. The main sand body has a porosity of 21%, but the net to gross ratio is only 0.3, which is not ideal. A low net gross ratio of 0.3 means that the potential reservoir section's quality has been rated as poor and the sandstones are typically very thin. The primary factor restricting permeability is a locally strong late cementation by dolomite (Kukulus, 2004).

Domingos (2018) conducted an analysis of reservoir unit predictions derived from seismic profiles and contrasted them with those associated with volcanic lithounits. The study identified several factors contributing to the unsuccessful discovery of economically viable quantities of recoverable hydrocarbons in wells. These factors often include the absence of essential elements within the petroleum system, as well as specific processes. Notably, the absence of a suitable reservoir or charge frequently emerges as a primary reason for such failures.

1.3 Location Map of the Study Area

The Walvis Basin is located south of the Walvis Volcanic Ridge, along the southern West Atlantic coast of Namibia, and covering an extensive area of approximately 105,000 km^2 (Kukulus, 2004).

The H-T field is an offshore field located within the Walvis Basin (Figure 2). The water depths across the field varies from less than 200 m to 1500 m. The four exploration wells pseudo-named HT1, HT2, H3, and HT4 due to Namibia's National Petroleum Corporation of Namibia (NAMCOR) confidentiality agreement were drilled.

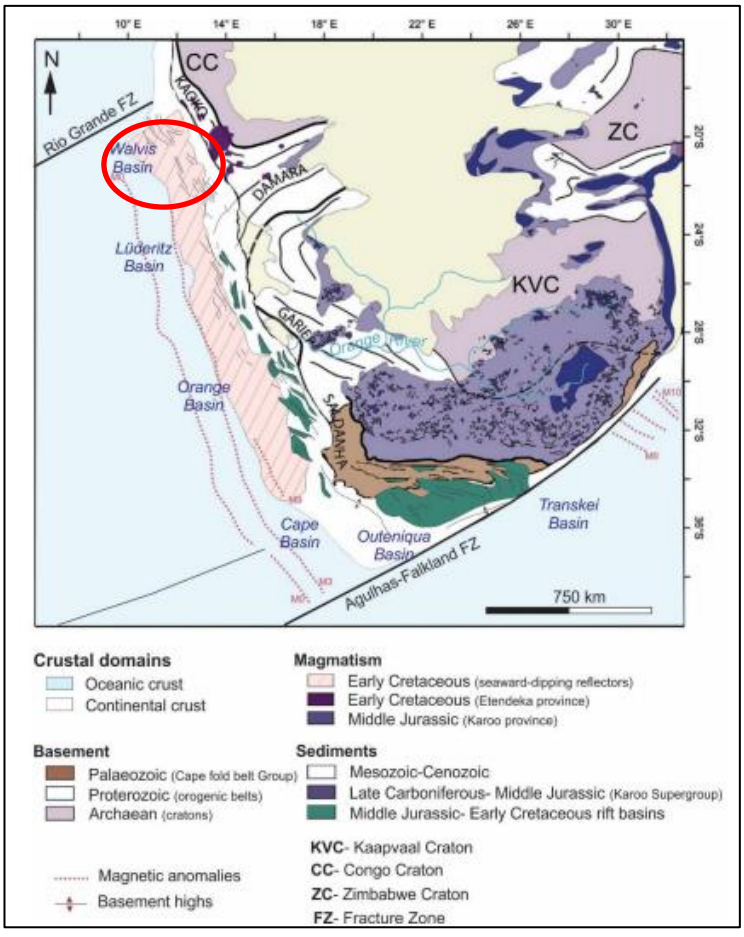

Figure 2: Location of the Walvis Basin (modified after Baby et al., 2018)

1.4 Statement of the Problem

Two exploration wells (Wingat and Murombe), have reduced the uncertainty on distribution of oil mature Aptian source risk in the Walvis Basin (Intawong et al., 2017). Both wells encountered thick Aptian restricted marine source rock above the Break-up Unconformity. The presence of light oil in the Wingat well, suggest that the Walvis Basin has a possible petroleum system. Despite the presence of hydrocarbon traces within the Wingat well, little is documented about petrophysical properties of reservoir rocks in the Walvis Basin.

1.5 Objectives of the Study

The aim of this study is to interpret the well log data and quantitatively evaluate the petrophysical properties to identify potential reservoirs for hydrocarbon accumulation with depth and thickness of the zones and to distinguish the interfaces of oil, gas, or water in the H-T field. The specific objectives include the following:

a) Identification of potential reservoir.

b) Petrophysical evaluation of log data.

c) Quantification of fluid in the reservoir.

CHAPTER 2: GEOLOGICAL SETTING

2.1 Regional Geological Setting

The South American and African plates were connected as a part of West Gondwana until the Jurassic Period. A regional rifting, accompanied by volcanism in the Late Jurassic and Early Cretaceous caused the drifting apart of the African and South American plates resulted in the formation of the South Atlantic Ocean (Séranne & Anka, 2005). The Namibian margin was formed during this process and is classified as a passive margin. The rifting of Gondwana was followed by initial faulting and the formation of the syn-rift basins characterized by grabens and half-grabens that trend sub-parallel to the present-day coastline. The four sedimentary basins from north to south are: Namibe, Walvis, Luderitz, and Orange Basin (Figure 3). As per the findings of Wildman et al. (2018), the stratigraphic composition preserved within the Walvis and Orange Basins is attributable to geological phenomena and sedimentary accumulation arising from erosional activities that shaped the topography of southwestern Africa.

The Walvis Basin is located off the northwest coast along the Namibian shoreline and covers an extensive area approximately 105,000 km^2. It lies south of the Walvis Volcanic Ridge (Figure 4) and bounded to the south by the Waterberg-Omaruru fault zone which represents a reactivated basement structure (Stollhofen, 1999). The Walvis Basin shows a wedge-shaped geometry typical of passive margin postrift sediments (Kukulus, 2004), and acted as the depocenter for sediments deposited from the Ugab

River since the late Early Cretaceous (Intawong et al., 2017). The basin is filled by shallow marine clayey siltstones topped by an organic-rich level (Hodgson & Intawong, 2013).

Figure 3: Structural framework of the south-western continental margin of Africa and south-western South America. The width of the South Atlantic is not to scale and was chosen arbitrarily in order to show both continental margins in one picture (adopted Schmidt, 2004)

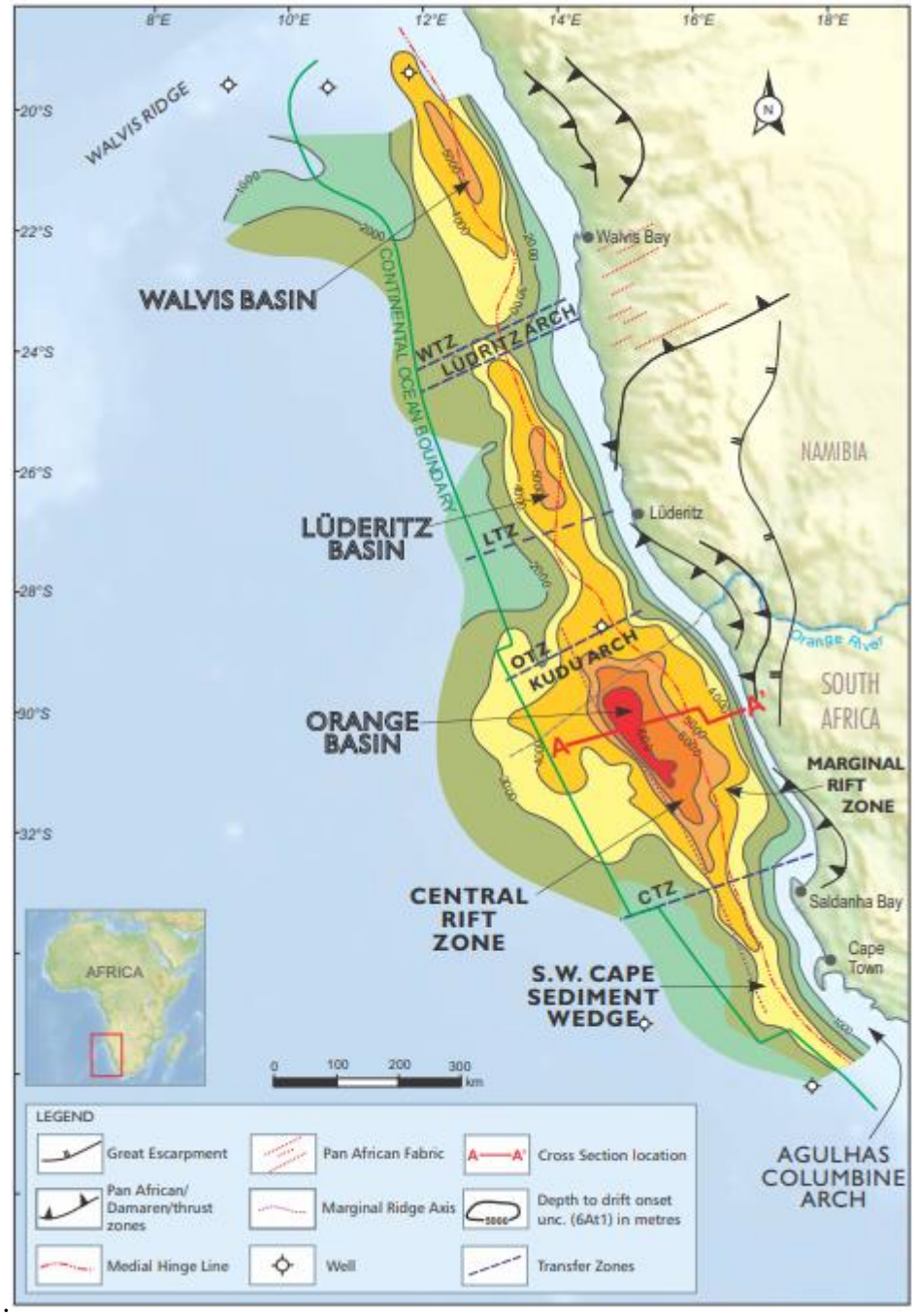

Figure 4: Structural Framework of Southwest Africa (Petroleum Agency South Africa, n.d.)

2.2 General Sequence Stratigraphy

The sequence stratigraphy of the Walvis Basin (Figure 5) is divided into syn-rift and

post-rift phases (Holtar and Forsberg, 2000; Baby et al., 2018). Syn-rift sequence comprises of layered units of continental volcanic rocks and siliciclastic sediments related to the emplacement of Etendeka lavas and onshore erosion (Wildman et al., 2020). The Late Hauterivian (132.9-129.4 Ma) breakup unconformity defines the boundary between the syn-rift and post-rift sequences (Baby et al., 2018; Light et al., 1993). The post-rift sequences comprise of the mid-Late Cretaceous and Cenozoic sequences of interbedded siltstone, claystones and minor sandstone interbeds deposited in a marine shelf, slope and basin environmental setting which provide evidence of post-rift erosion (Baby et al., 2018; Clemson et al., 1997; Holtar & Forsberg, 2000). The Late Cretaceous succession shows fault structures associated with episodic gravitation collapse during the uplift of the onshore domain (de Vera et al., 2010). Several major unconformities are observed in the lower Campanian, top Maastrichtian, middle Oligocene and upper Miocene (Baby et al., 2018).

The Ugab River has provided the sand rich sediments into the Walvis Basin since the late Early Cretaceous time (Intawong et al., 2017). This river has its source in the South African plateau of the Congo craton and Damara belt and crosses the marginal buldge, a noticeable large-scale feature, close to the outcrops of the 132 to 125 Ma Etendeka flood basalt (Dauteuil et al., 2013). The Etendeka volcanic province contributes only ~4% of the present day of the sand in sandy beaches of the Skeleton Coast (Garzanti et al., 2014). The Walvis Basin experienced high sediment input (23.15 x 10^4 km) during the mid-Late Cretaceous (Baby et al., 2018).

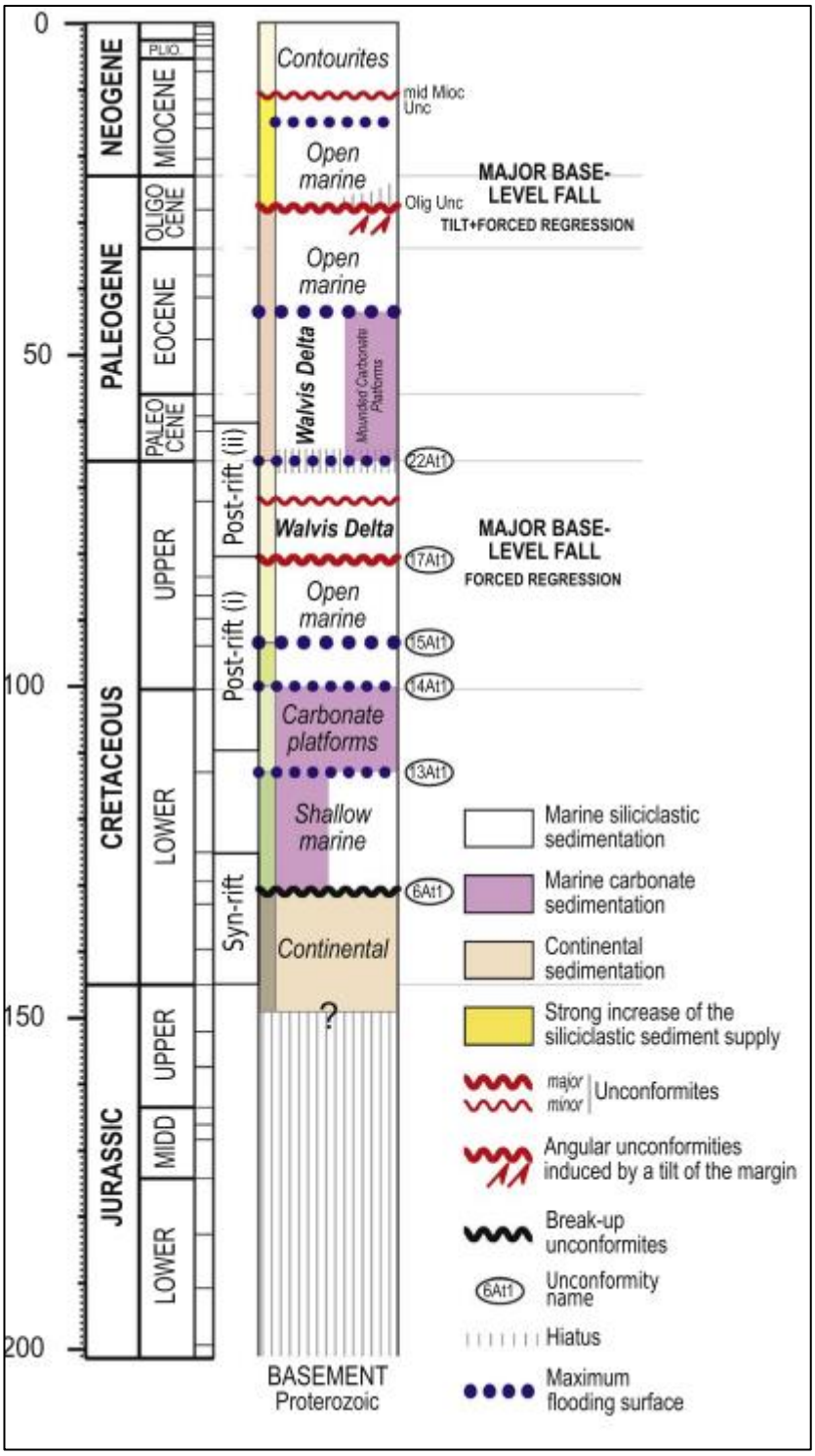

Figure 5: Representative stratigraphic column of the Walvis Basin (adopted from Wildman et al., 2020 modified after Baby et al., 2018)

2.3 Petroleum Systems of the Walvis Basin

The complex interplay of geologic processes contributes to the genesis and accumulation of hydrocarbons, constituting what is known as a petroleum system (Magoon & Dow, 1994). Such a system comprises several key components, including an organic-rich source rock, a reservoir rock capable of storing hydrocarbons, a seal or cap rock to prevent their escape, and a structural or stratigraphic trap that confines them. Additionally, migration pathways and timing are essential aspects of this system. Despite being relatively unexplored, the Walvis Basin has yielded promising results from limited drilling activities, affirming the presence of a viable petroleum system within the basin (Bray et al., 1998).

2.3.1 Source Rocks

The exploration drilling conducted at the Wingat-1 and Murombe-1 wells in the offshore region of Namibia has provided conclusive evidence of the presence of an oil-prone source rock throughout the Walvis Basin (Cole, 2021). This comprehensive analysis has identified three distinct source rocks distributed across various stratigraphic intervals, including the Cenomanian-Turonian, Aptian, and Syn-Rift horizons.

The Cenomanian-Turonian marine anoxic system is a widely distributed good quality source rock with an average 4% Total Organic Content (TOC) and is encountered by most wells drilled in the basin (Utjavari, 2019). The only potential risk for this source

rock is its maturity demonstrated in Wingat-1 and Murombe-1 wells (Mello, 2022).

The Barremian-Aptian Kudu Formation is the most important and richest interval. The Wingat-1 and Murombe-1 showed a very thick interval (100-200 m), marine black shale, containing TOCs of 2-3.5% (Mello, 2022). According to Mello (2012), the vitrinite reflectance (%Ro) values of ~0.85-0.90%, for both wells indicated the entire Kudu Formation section was within the late peak oil-generating window, therefore suggesting that most of the original organic-rich potential had been converted in hydrocarbons. Interpretation of regional well and 2D seismic data in the Namibia and South Africa margin suggests that the Barremian-Aptian source rock is present over wide parts of offshore Namibia, as far north as the Walvis Ridge and in South Africa (Hedley et al., 2022).

The Syn-rift section is only observed on seismic but has never been penetrated by wells drilled in Namibia (Utjavari, 2019).

2.3.2 Generation and Migration

Oil generation is anticipated from the Turonian, Cenomanian, and Aptian shales located beneath and in downdip proximity to the lead traps, with migration occurring along faults intersecting both the source rock and the lead section. The leads identified on seismic data comprise structural and fault traps, as well as stratigraphic traps with shale layers serving as seals. These seals, however, have not been observed in the

limited number of wells drilled within the basin, and the structural features are delineated based on seismic time maps (Utjavari, 2019).

2.3.3 Reservoir Rocks

The reservoirs comprise marine-deposited sandstones found within channel-fan complexes on the continental slope, with anticipated high-quality reservoir characteristics anticipated particularly at the Cenomanian and Santonian levels (Utjavari, 2019). Carbonate reservoirs may also be present (Mello, 2022). The reservoir rocks found in the Murombe-1 and Wingat-1 wells were identified as Albo-Cenomanian confined channel turbidite complex, characterized by sub-angular coarse- to fine-grained sand, 19% average porosity and Barremian transitional carbonates (Mello, 2022). Barremian to Aptian synrift reservoirs consist of eolian, lagoonal and marine sandstones are observed in the Kudu gas field.

The significant findings of the recent drilling in the Walvis Basin were the discovery of light oil (41° API, GOR 1,193 scf/bbl) in the lower Cretaceous Albian, sandstones turbidites, with very good permo-porosity values, in the Wingat-1 well (Mello, 2022).

2.3.4 Traps and seals

Structural, fault and stratigraphic traps with shale layers as a seal form the leads (Lencioni, 2016).

CHAPTER 3: PETROPHYSICAL PARAMETERS

Wireline log data, including Gamma Ray (GR), spontaneous potential (SP), caliper (CL), density (RHOB), neutron (NPHI), photoelectric effect (PEE), and resistivity logs (comprising deep resistivity (LLD), shallow resistivity (LLS), and medium resistivity (ILM)), are utilized for the calculation of petrophysical parameters. The are several software such as Techlog, Petrel and Interactive Petrophysics (IP) that can be used to integrate all available wireline logs to interpret and compute the input of the different petrophysical properties to enable a realistic and accurate formation evaluation. Formation evaluation is the process of using borehole measurements to calculate the characteristics of subsurface formations (Helander, 1983).

To ascertain the reservoir properties of formations, it is imperative to acquire and assess petrophysical parameters. These parameters encompass lithology, shale volume, porosity, water saturation, hydrocarbon saturation, permeability, net pay, and gross thickness.

3.1 Lithology

The lithology identification is crucial for reservoir characterization because all the petrophysical parameters, such as porosity and permeability depend on facies type. Likewise, fluid saturations directly depend on facies types (Amigun & Odole, 2013). Lithology in wells can be identified by using gamma ray (GR) log, photoelectric factors (PEE) (Table 1). The lithology and mineral composition of the reservoir are determined using several types of cross plots, such as:

a) Neutron - density lithology cross plot

b) Neutron – sonic lithology cross plot

c) M-N lithology cross plot

d) Matrix identification (MIS) cross plot

e) Density – photoelectric effect – gamma ray cross plot

Table 1: Photoelectric parameters for common lithology in sedimentary rock (Nwankwo et al., 2014)

Lithology	Sandstone	Dolomite	Shale	Limestone	Anydrite
PEE Value barns/electron	1.8-2	3.14-4	1.8-6.5	5	5

3.2 Reservoir

The reservoir, distinguished by its potential for economic interest, serves as the sole zone capable of accumulating hydrocarbons or water (Senosy et al., 2020). A favorable reservoir rock is characterized by its porosity, permeability, and hydrocarbon content (Ellis and Singer, 2007). Sandstone reservoirs typically exhibit low radioactivity due to minimal radioactive element content, making gamma ray logs useful in their identification. Additionally, reservoir zones typically demonstrate higher resistivity values compared to non-reservoir zones, as indicated by resistivity logs. Neutron and density log further aid in identifying reservoir rock through the presence of neutron-density crossovers (Lyaka et al., 2018; Nwankwo et al., 2014).

3.3 Fluid

Delineating the interval zone and identifying the fluid type within the reservoir rock is essential, as reservoirs may contain hydrocarbon (oil and gas), non-hydrocarbon fluid (water), or a combination of both (Senosy et al., 2020). Hydrocarbon-bearing reservoirs typically exhibit porous characteristics with resistivity values higher than those of water-bearing zones (Crain, 2016).

The resistivity log and neutron–density log can be employed to identify hydrocarbon and non-hydrocarbon-bearing intervals. Hydrocarbons exhibit higher resistivity compared to water-bearing intervals due to their lower conductivity. Neutron and density crossover analyses indicate distinct characteristics of gas and oil zones. Gas zones typically show a wider negative separation owing to their low density and hydrogen index, while oil zones display relatively lower negative separation attributed to their higher density and hydrogen index compared to gas.

3.4 Volume of shale (Vsh)

Estimating shale volume is essential for assessing the potential of zones as reservoirs. This determination is pivotal in petrophysical interpretation as it enables the calculation of formation porosity, fluid content, and overall rock quality.

Clay can have various effects on the reservoir quality such as reduced porosity and

permeability (Opuwari, 2010). It may also change the electrical properties of the reservoir in which case it needs to be accounted for in calculation fluid saturations.

As highlighted by Hilchie (1978), the primary impact of shale in a formation is to diminish the resistivity contrast between oil or gas and water. The shale volume, expressed as a decimal fraction or percentage, is denoted as V*shale*.

Shale Volume can be estimated from numerous logging measurements. This can be achieved with single measurements such as gamma ray, Spontaneous Potential, neutron and resistivity or it can be done with a combination of measurements such as density-neutron, density-sonic and sonic-neutron.

Single indicator which is gamma ray can be used in Water or Oil Based mud systems to provide good distinction between shale and non-shale intervals. Corrected Gamma Ray can remove the influence of uranium to give a better indication of clay/shale content. However, GR can be affected by mineralogy such as hot sands (sands that have high concentrations of potassium), can be affected by the presence of Potassium in Water Based Muds, and or if other nuclear tools are used prior to the GR high responses on the Gamma Ray tool may be seen due to activation of the formation.
Furthermore, for precise reservoir lithological description crucial for reservoir management, the Density-Neutron method can be employed (Rider, 2002). Clay volume is ascertained from density and neutron porosity curves plotted against each

other on a crossplot, with both curves exhibiting a linear response to escalating clay content. Density-Neutron measurements are unaffected by non-clay radioactive minerals and are not sensitive to Potassium in the drilling mud. However, they can be influenced by borehole size and the presence of gas. Tools utilizing this method may be deployed as frequently as Gamma Ray tools due to constraints on nuclear sources.

3.5 Net to Gross ratio (h/H)

Establishing net pay thickness is crucial for determining the original hydrocarbon in place. Net To Gross (NTG) represents the ratio of the thickness of hydrocarbon-bearing sand to the total thickness of the sand formation (Nwankwo et al., 2014), providing insight into the volume of shale present in the reservoir. The net reservoir thickness (h) can be estimated using the following formula:

$h = H\text{-}h_{shale}$,

Where *H*=The gross reservoir thickness, h_{shale}=The thicknesses of the shale and Net/Gross=h/H.

3.6 Porosity

Porosity, denoted by the Greek letter Phi (Φ), represents the ratio of pore space to the bulk volume of the rock, serving as an indicator of the potential storage space for fluids (Senosy et al., 2020) . It can be expressed either as a percentage (%) or a decimal ratio of volumes (v/v).

It is crucial to differentiate between Total porosity (PHIT) and Effective porosity (PHIE). Total porosity is defined as the ratio of all pores' volume to the bulk volume of substance, whether all pores are related or not (Rider, 2002). Effective porosity represents the ratio of the volume of only interconnected pore in a material to the total volume of reservoir rock (Rider, 2002). The capillary bound water is attached to matrix grains by interfacial tension and is not moved under normal production conditions. The effective porosity can be deduced by introducing shale volume into the equation. Porosity is an important component in the evaluation of the stock tank oil initially in place.

3.7 Water Saturation

Water Saturation (S_w) denotes the fraction of the porosity occupied by a specific fluid within a formation (Holstein & Warner, 1994). It is quantified as a percentage (%) or decimal ratio of volume (v/v). In a formation, pores may be filled with gas, oil, or water, and the sum of the saturation of all fluids must total 100%. A water saturation value of one (1) indicates that the pore volume is entirely filled with water.

If the pore volume is entirely filled with water, the water saturation is one i.e., 100%. If the pore volume is a ¼ filled with water the S_w is 0.25 and the remainder is assumed to be another fluid such as hydrocarbon, or oil or gas saturation (S_h, S_o or S_g respectively).

In the oil and gas rich section a small volume of water will always be present as clay

or capillary bound water. Therefore, pore volume is never 100% hydrocarbon saturated. The original formation water that was present would have been displaced by the migrating hydrocarbons due to capillary forces between the formation water and the grains, not all of it could be displaced (McDonald, 2016). This minimum S_w value is referred to as Irreducible Water Saturation (S_{wirr}).

Assessing water saturation is essential as it facilitates the calculation of hydrocarbon saturation. Various models exist for determining water saturation in non-clean or shale-bearing sandstone reservoirs. The Archie equation, for instance, assumes that the matrix is non-conducting in clean sands, exploring the relationship between porosity, formation water resistivity, and true formation resistivity concerning water saturation. However, in non-clean or shale-bearing formations, as well as heterogeneous formations, the Archie equation may not be as effective. The Simandoux model, on the other hand, accounts for additional conductivity stemming from clay (Zhang & Xu, 2016). The Indonesian equation was developed by Poupon and Leveaux (1971) to account for the high amount of shale and freshwater formations contained in Indonesia reservoirs. The equation was developed by using computer-made cross-plots to determine the relationship between the value of water saturation and the value of the true resistivity of the formation (Sam-Marcus et al., 2018).

3.8 Hydrocarbon Saturation

Hydrocarbon saturation (Sh) is the percentage of pore volume in a formation occupied by hydrocarbon. On the contrary, the residual hydrocarbon saturation is the differences between unity and water saturation in the flushed interval (Rider, 1986). Both water saturation (Sw), as well as water saturation of the flushed zone (Sxo), can be applied to calculate the amount of movable hydrocarbon (Baban et al., 2018).

3.9 Permeability

Permeability (k) is a measure of the ease with which fluids move through a porous medium. Grain size is a key controlling factor on rock permeability. Where there is more than a single fluid present, the permeability of the rock to given fluid will be reduced and this is known as effective permeability (Ke).

$$Q = \frac{KA\Delta P}{\mu L}$$

Where Q – volumetric flow rate, A – cross-sectional area, P/l – pressure drop, μ - viscousity of fluid.

Permeability is measured in Darcy, which is too large for flow in a reservoir, so millidarcies (mD) or microdarcy (μD) in tight rocks is more appropriate for reservoirs. In general, a rock with a K value greater than 1mD is considered a reservoir rock. 10 – 100 mD – high permeability. 100 – 1000 mD – very high permeability values.

Several methods exist for estimating permeability using wireline tools, with the Timur

and Morris equations commonly applied in calculating permeability for carbonate reservoirs. These equations can serve as empirical tools to predict reservoir permeability in cases where core data for the reservoir is unavailable (Nkwanyang et al., 2018).

3.10 Net Pay

To assess reservoirs, it is essential to determine net pay and gross thickness, wherein net pay signifies the thickness of the porous and permeable zone within an evaluated formation containing economically viable hydrocarbon quantities. The net-to-gross ratio (N/G %) is defined as the ratio between the thickness of net pay and the thickness of the total pay zone.

Net pay thickness is the most critical factor to calculate hydrocarbon in place because it affects reservoir management and reservoir productivity (Katz & Thompson, 1986).

CHAPTER 4: MATERIALS AND METHODS

In this study, wireline log data was utilized to conduct qualitative and quantitative analysis of the petrophysical properties of potential reservoir intervals employing the Senergy Interactive Petrophysics (IP) software. This software encompasses programs for the interpretation of all petrophysical characteristics, encompassing environmental corrections, statistical, petrophysical, and lithological analyses utilizing various equations, empirical relations, and charts. Figure 6 outlines the workflow, summarizing the sequential steps undertaken to characterize the H-T Field in the Walvis Basin, Namibia.

4.1 Acquisition of Raw Data

The wireline log data utilized in this study were provided by the National Petroleum Corporation of Namibia (NAMCOR). The drilled boreholes include HT1, HT2, HT3, and HT4, each equipped with main logs such as gamma ray (GR), spontaneous potential (SP), caliper (CL), density (RHOB), neutron (NPHI), photoelectric effect (PEE), and resistivity logs (deep resistivity (LLD), shallow resistivity (LLS), medium resistivity (ILM)). These logs were furnished in soft copy Log ASCII format (LAS files) as detailed in Table 2, and were utilized for the computation of petrophysical parameters, given the unavailability of core data.

Reports on the four wells were made available by NAMCOR. These reports are largely biostratigraphic studies. No petrophysical characteristics report obtained.

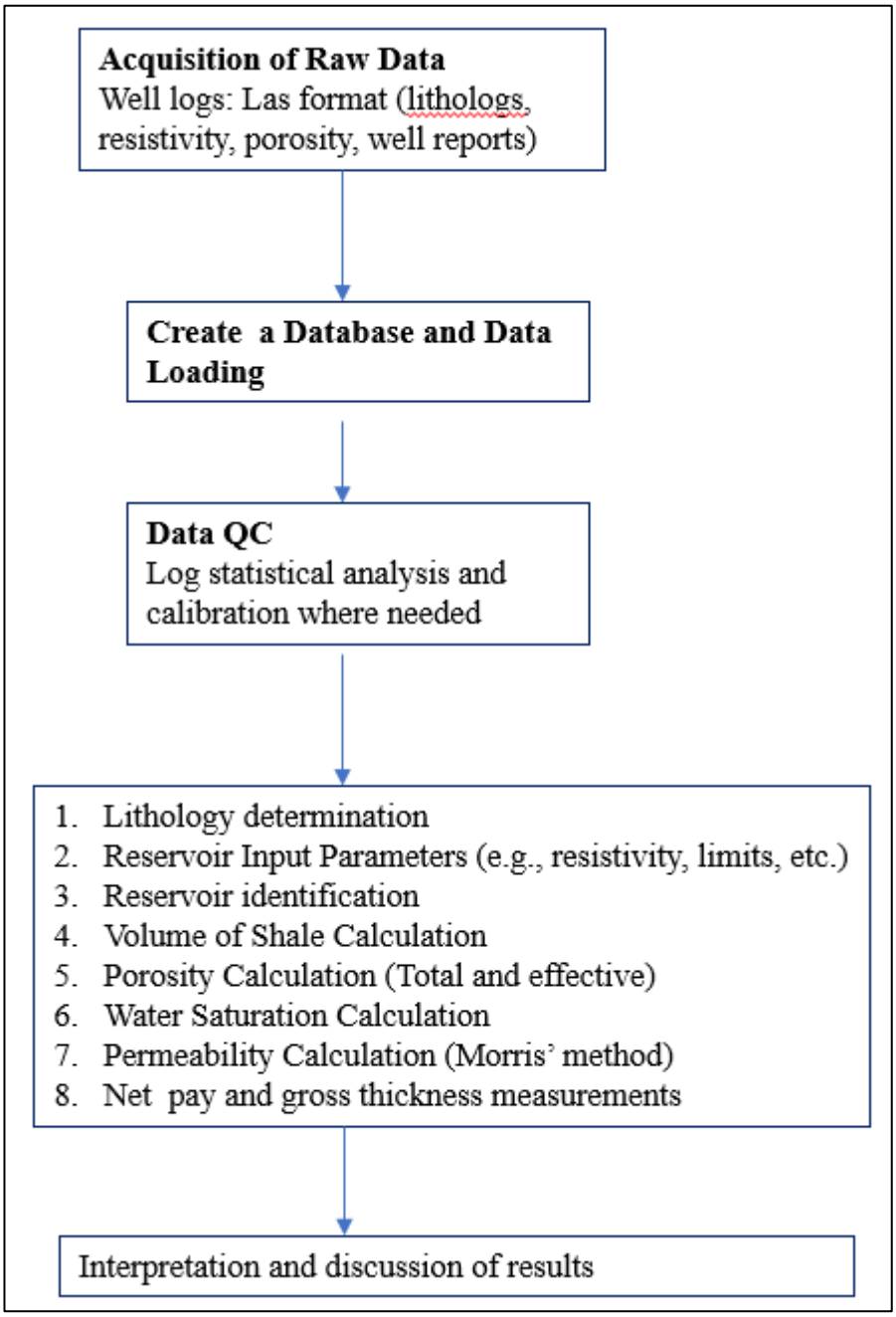

Figure 6: Simplified workflow adopted to characterize H-T field, offshore Walvis Basin, Namibia.

The Interactive Petrophysics (IP) software was used to integrate all the available data to interpret and compute the input of the different petrophysical properties to deliver a formation evaluation.

Table 2: The available open hole wireline logs and surface temperature (ST), bottom hole temperature (BHT) for the four studied wells

Logs	**Well**			
	HT1	HT2	HT3	HT4
Gamma Ray (API)	*Y*	*Y*	*Y*	*Y*
Caliper	*Y*	*Y*	*Y*	*Y*
Sonic	*Y*	*Y*	*Y*	*Y*
Spontaneous potential	*N*	*N*	*Y*	*N*
Density (gm/cm^3)	*Y*	*Y*	*Y*	*Y*
Neutron Porosity	*Y*	*Y*	*Y*	*Y*
Photoelectric effect	*Y*	*Y*	*N*	*N*
Deep resistivity	*Y*	*Y*	*Y*	*Y*
Medium resistivity	*Y*	*Y*	*Y*	*Y*
Shallow resistivity	*Y*	*Y*	*Y*	*Y*
Surface temperature (^{o}C)	*58.76*	*8.2*	*4*	*4*
Bottom hole temperature (^{o}C)	*93.29*	*72*	*133*	*133*

Y and N stands for availability and non-availability of data respectively

4.2 Creation of Database

Digital data were received from NAMCOR in LAS format files at different runs across the wells. The database was created in the Interactive Petrophysics software, and the logs were loaded into.

4.3 Data Quality Check

Several issues were encountered with logs that necessitated editing before their utilization for qualitative analysis, including depth shifting/matching, borehole environmental corrections, smoothing/des-spiking/noise removal, and merging/splicing of curves, among others. Following the editing process, curve normalization is performed, which involves a mathematical adjustment to account for differences among data from different sources, thereby establishing a common baseline for comparison.

The Gamma ray logs for the four wells were normalized based on the method and guidelines reported by (Shier, 2004). Well HT1 was chosen as the reference well for normalization because it has the lowest mean average GR of 60 API. A shale cut-off value of 60 API was used for all the four wells (HT1 to HT4) to establish the sand base line for reservoir discrimination.

4.4 Lithology Determination

Gamma ray logs were employed to identify the reservoir units. A shale cut-off value of 60 API was used for both wells, to establish the sand base line and discriminate the reservoir units based on the lower GR unit readings.

To enable accurate reservoir lithologic description relevant for reservoir management,

Sonic–Density, Neutron–Density, M–N crossplots, as well as mineral identification (MID) plots were used to determine reservoir lithology and associated constituent rock minerals. This allowed the determination of reservoir lithologies and constituent mineralogy.

4.5 Potential Reservoir Identification

Reservoir rock was identified using the interpretation of the available gamma ray log. Since the sandstone reservoir shows very low radioactivity due to the low content of radioactive elements (Rider & Kennedy, 2011), a shale cut-off value of 60 API was used to establish the sand base line and thus discriminate reservoir units based on the lower GR readings. GR minimum represents clean sands and was called sand line. Whilst GR maximum was assumed to represent 100% shale and called shale line.

Resistivity logs were also used because reservoir zones exhibit relatively higher resistivity values than non-reservoir zones. Reservoir rock may also be marked by the presence of neutron–density crossover (Nwankwo et al., 2014).

4.6 Fluid Identification

The resistivity log and neutron-density log were employed to differentiate between hydrocarbon-bearing and non-hydrocarbon-bearing intervals. Hydrocarbons exhibit higher resistivity compared to water-bearing intervals due to their lower conductivity. The deep resistivity log was specifically utilized to identify hydrocarbon zones, with

zones demonstrating resistivity values exceeding 4 OHMS being classified as hydrocarbon-bearing. Low resistivity pay hydrocarbon zones have been documented within the resistivity range of 4 OHMS in fine-grained lithologies (Afizu, 2013).

The neutron and density log (density and neutron crossover) were used to discriminate the hydrocarbon types, the gas zone is expected to show a wider negative separation due to low density and low hydrogen index of gas, while the oil zone is also expected to show relatively low negative separation because of relatively high density and hydrogen index compared to gas.

4.7 **Clay Volume (Vclay) or Shale Volume (Vsh) Determination**

To differentiate between reservoir and non-reservoir rock, a comprehensive analysis of clay volume was conducted utilizing multiple clay indicators, including gamma ray, resistivity, and density/neutron curves. The measurement of the gamma ray (GR) index is a crucial step in defining shale volume via the GR log (Asquith & Krygowski, 2004). Shale volume within the delineated reservoir unit was assessed to facilitate the estimation of effective porosity, employing the gamma ray curve, and utilizing a non-linear Stieber equation tailored for Cretaceous rock.

$$V_{sh}\ \text{Steiber}\ (V_{sh}\_gr\_s) = \frac{0.5 \times V_{sh\_gr\_l}}{1.5 - V_{sh\_gr\_l}}$$

Where Vsh_gr_1 is ($GR-GR_{CL}$ / $GR_{SH}-GR_{CL}$), GR = gamma ray reading in zone of

interest, GR_{CL} = Gamma ray log reading in 100% clean zone, GR_{SH} = Gamma ray log reading in 100% shale.

4.8 Porosity Determination

The Porosity and Water Saturation interpretation module in IP software was used to calculate porosity (PHI), water saturation (SW), flushed zone water saturation (SXO), matrix density (RHOMA), hydrocarbon density (RHOHY), and wet and dry clay volume (VWCL and VDCL). Formation temperature of each hole was provided as part of the data suit.

4.9 Determination of the Water Saturation (Sw)

The Porosity and S_w module within IP software was used to interactively select parameters for the calculation of the porosity and from which a water saturation was derived. Saturated Water for identified reservoir zones was estimated based on Simandoux water saturation formula. This formula takes consideration of the impact of the clay volume, enabling easy determination of the hydrocarbon saturation (Chongwain et al., 2019; Zhang & Xu, 2016).

4.10 Permeability Determination

To assess the potential fluid productivity of a zone, the permeability of the rocks was assessed. In the absence of core data for the reservoir, empirical calculations were employed to predict permeability within the reservoir. The Morris Biggs oil equation

was utilized for this purpose, employing wireline logs to predict permeability. The constants used for calculating permeability in Interactive Petrophysics are as follows: a = 62500, b = 6, and c = 2.

4.11 Net Pay or Net Reservoir Quantification

Using the formation parameters, a determination of how much rock contains producible hydrocarbon was made. Cutoffs are formation parameter values that were used to eliminate sections of an entire rock volume that do not contribute to the final reservoir evaluation. The Cutoff and Summation module of the IP software was used to derive reports on Net Pay and Net Reservoir and any additional user derived reports. Cutoff values were established for the volume of clay, effective porosity and water saturation curves based on available data from Orange Basin of South Africa (Opuwari, 2010). The cutoff values adopted are 0.4, 0.1 and 0.65 respectively. Based on these cutoff values, pay zones were delineated.

CHAPTER 5: RESULTS AND INTERPRETATION

This chapter provides an overview of the reservoir parameters pertaining to lithologic

properties, reservoir intervals, volume of shale, porosity, saturation, and permeability derived from the analysis of data from the four wells. The results obtained are presented through various formats including well-log responses, lithologic sections, cross plots, and tables, among others.

5.1 Lithological identification

The petrophysical analysis of well logs in HT field was based on low gamma ray response, photoelectric effect values and neutron-density crossover. The identified main lithology of the wells consists of three types of lithology, namely: sand, shale, and siltstone.

The generated cross-plots indicate that the main lithology is sandstone and shaly sandstone (Figure 7). The two sand units were distinguished as two different potential reservoir zones based on eliminating thick shale beds between reservoirs and low value of deep resistivity to reduce the effect of both increasing shale volume and high-water saturation when calculating other petrophysical parameters.

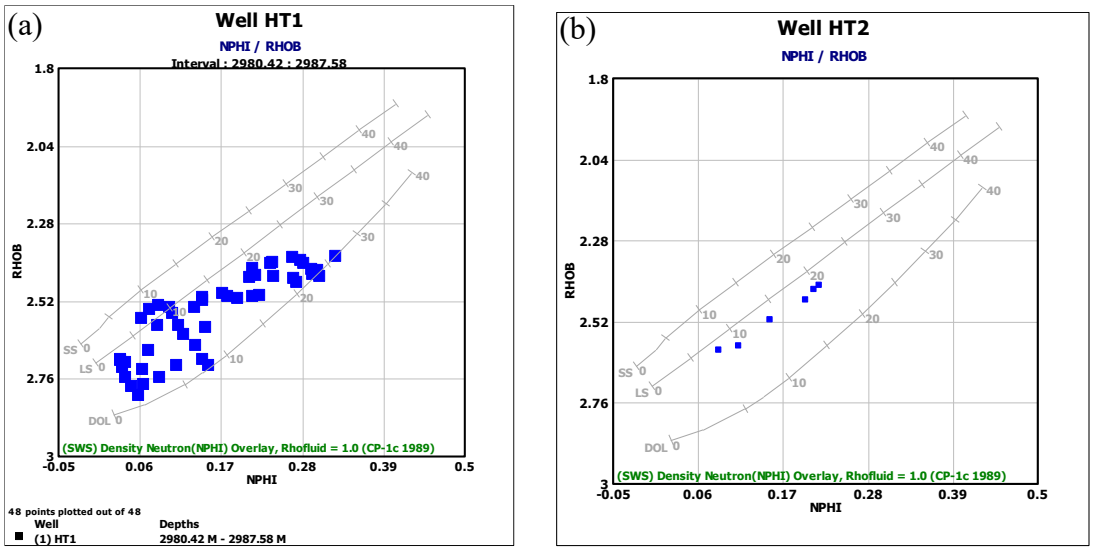

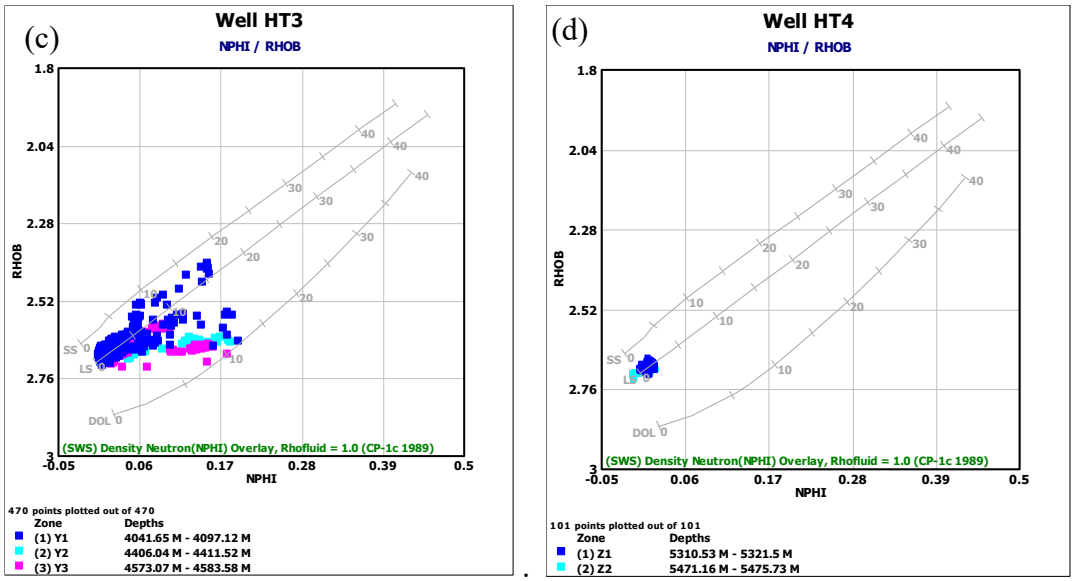

Figure 7: (a) Density-neutron cross-plot of the potential reservoir in Well HT1, (b) Density-neutron cross-plot of the potential reservoir in Well HT2, (c) Density-neutron cross-plot of the potential reservoir in Well HT3, (d) Density-neutron cross-plot of the potential reservoir in Well HT4

5.2 Reservoir identification and evaluation

Seven reservoir units were identified based on the gamma ray log response of the four wells. These zones were characterized by the low gamma ray response, high porosity, neutron-density crossover, and high resistivity values.

5.2.1 Well HT1

In Well HT1, reservoir W1 was identified between 2980.57 m to 2987.73 m with gross

thickness of 7.16 m and an average gamma ray response of 60 API (Figure *8*). On a gamma ray histogram for W1 reservoirs, considerable point plotted beyond 60 API, suggesting that this reservoir is dirty or shaly in terms of clay content. The gamma ray log over this zone appears blocky (aggrading) with occasional stringers of high gamma ray values interpreted to be shale.

Deep resistivity measurements peak at a maximum of 12 OHMs. As indicated by Chongwain et al., (2019), deep resistivity values exceeding 4 OHMs are indicative of hydrocarbon presence. Notably, low-resistivity pay hydrocarbon zones have been documented within the 4 OHMs resistivity range, particularly within fine-grain lithologies (Afizu, 2013).

Neutron and density logs for W1 showed no observable crossover or "ballon effect" suggesting the occurrence of oil as the hydrocarbon phase. However, W1 reservoir contains no producible hydrocarbons (i.e. no pay zone), despite the low gamma ray readings and high resistivity readings. According to Zhu et al. (2018) this is a characteristic of calcareous interbeds which typically exhibit unique characteristics of low natural gamma less than 80 API and higher resistivity than any other sandstone. W1 reservoir possibly symbolizes a calcareous interlayer in which isolated thin sand layer was enveloped in mudstone and the entire sand was cemented by carbonate resulting in a tight reservoir.

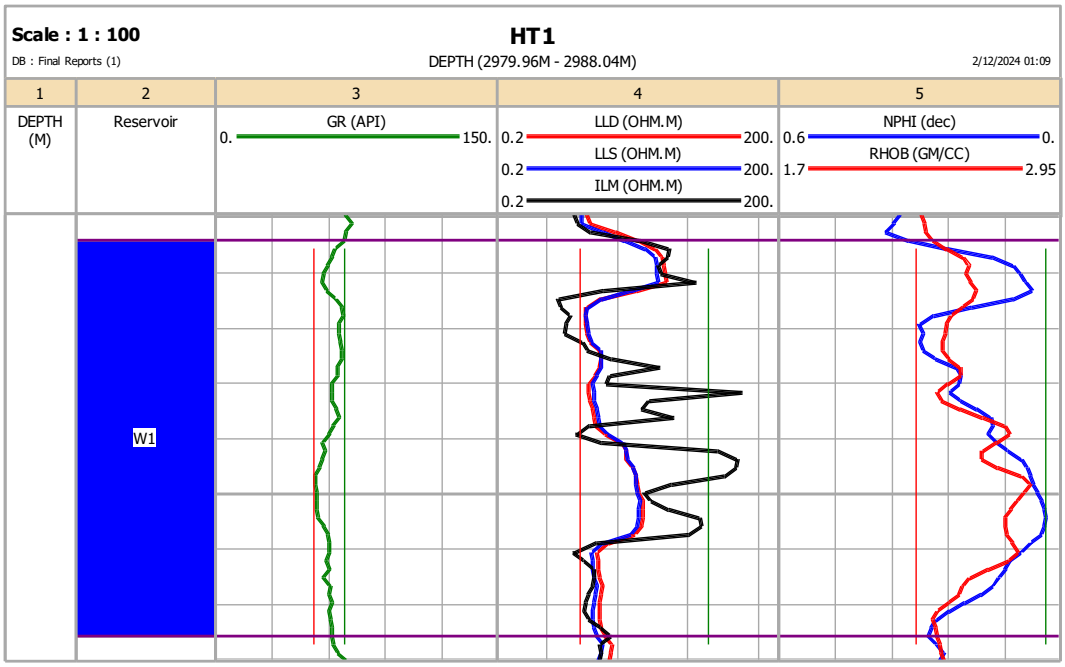

Figure 8: The interval depth with the composite log response of the potential reservoir zone in HT1 well

5.2.2 Well HT2

In Well HT2 (Figure *9*) a thin reservoir X1 was delineated from 3740.66 and 3741.72 m with a gross thickness of only 1.07 m and average gamma ray of 63 API. The gamma ray histogram for reservoir X1 revealed considerable points plotting beyond 60 API, indicating that the reservoir is dirty or shaly in terms of clay content.

The deep log resistivity readings reach a high of 7.9 OHMS; demonstrating a possibility of oil trapped within the stringers of sands. Reservoir X1 contains oil with an average hydrocarbon saturation of 67% and a net-to-gross of 0.143. The average volume of clay (Vclay) value of 0.38 v/v is way above the damaging limits of 0.15 v/v

(Hilchie, 1978), that can affect water saturation and free flow of fluid. The average porosity is 14%, with a permeability of 4.63 md, hence, porosity and permeability of reservoir X1 are both poor (e.g. Rider, 1986).

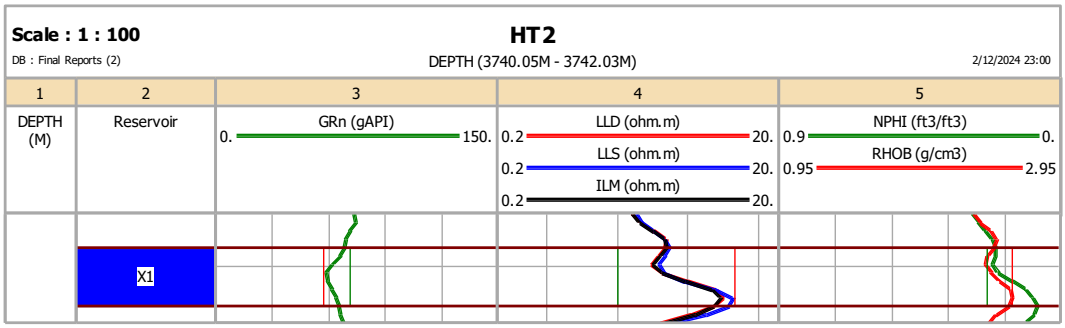

Figure 9: The interval depth with the composite log response of a potential reservoir zone in HT2 well

5.2.3 Well HT3

In Well HT3, three reservoirs' bodies were identified including Y1 encountered between 4041.65 and 4097.12 m, Y2 encountered between 4406.34 and 4411.37 m, while the third Y3 was encountered between 45703.07 and 4583.58 m with gross thicknesses of 55.47 m, 5.03 m and 10.52 m respectively (Figure *10*). The average gamma ray values over these reservoir bodies are 30 API, 36 API and 41 API over Y1, Y2, and Y3 respectively. The gamma ray histogram for Well HT3 reservoirs indicated that all points clustering below 60 API revealing that all the reservoirs are clean in terms of clay content.

Analysis of deep resistivity log data indicates that:

- Reservoir Y1 is peaking at 100 OHMs with an overall average of 38 OHMs;
- Reservoir Y2 has a maximum 66 OHMs and an overall average of 30 OHMs; and
- Reservoir Y3 has a maximum of 86 OHMs and an overall average of 34 OHMs.

A cross-plot of the neutron and density logs for Y1, Y2 and Y3 showed no observable "balloon effect" ruling out the occurrence of gas as the hydrocarbon phase.

Reservoir Y1 is characterized by water, exhibiting an average water saturation of 54% and a net-to-gross ratio of 0.01. Additionally, the average volume of clay (Vclay) is determined to be 0.05 v/v, which falls below the detrimental threshold of 0.15 v/v as outlined by Hilchie (1978). The average porosity of the water-bearing reservoir is calculated at 13%, accompanied by a permeability of 0.06 millidarcy (md), indicating poor porosity and permeability properties within the reservoir.

Reservoir Y2 contains water with an average water saturation of 64% and a net-to-gross of 0.26. The average volume of clay (Vclay) value of 0.08 v/v is below the damaging limits of 0.15 v/v (Hilchie, 1978). The average porosity for the water bearing reservoir is 12%, hence the reservoir porosity is poor according to a qualitative evaluation of porosity adopted from Rider (1986). An average permeability of 0.23 md was calculated for this reservoir, which is poor to permit free flow of fluid.

Reservoir Y3 contains water with an average water saturation of 64% and a net-to-gross of 0.46. The average volume of clay (Vclay) value of 0.12 v/v is below the damaging limits of 0.15 v/v (Hilchie, 1978). The average porosity is 12%, with a permeability of 0.02, which is poor to permit free flow of fluid.

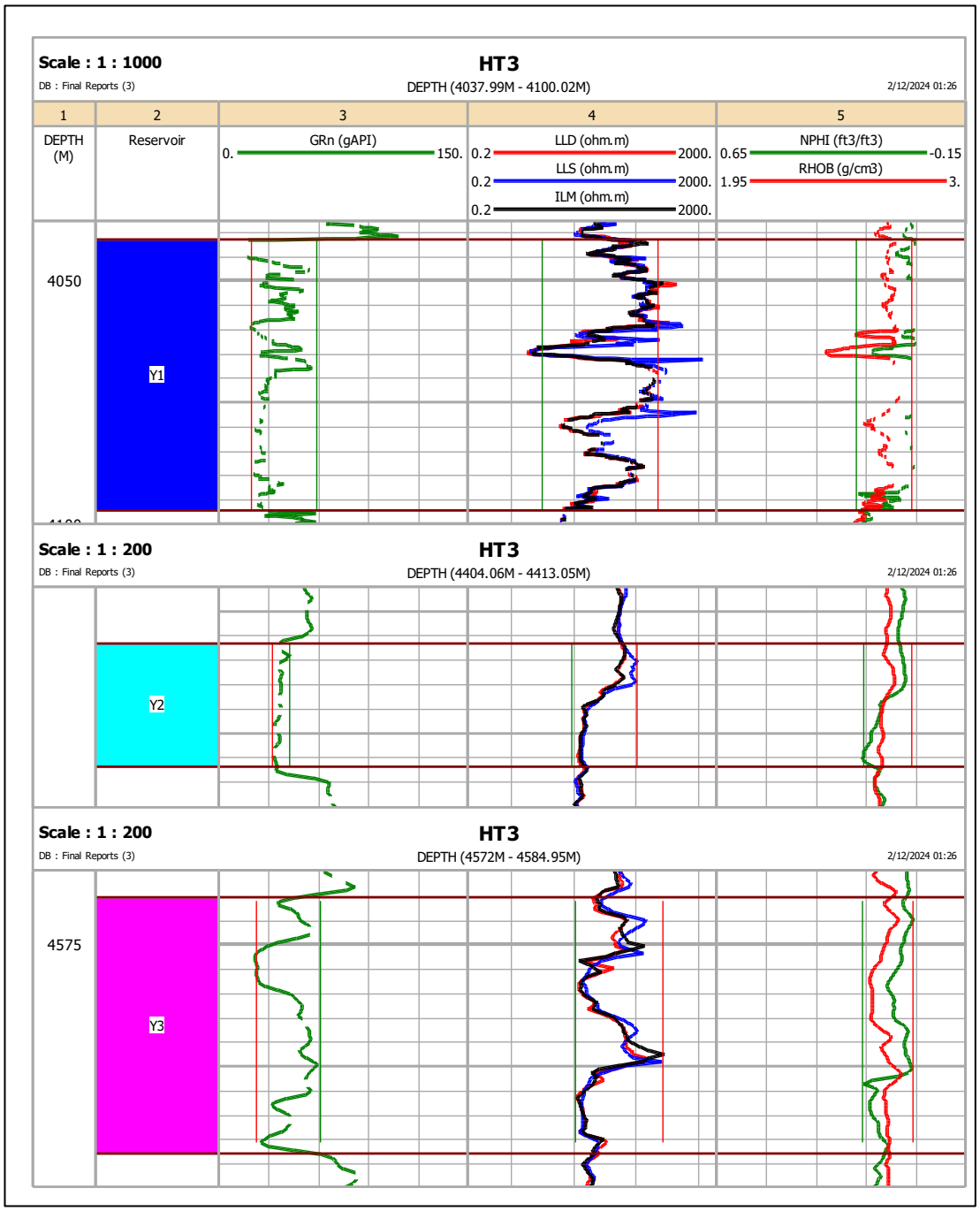

Figure 10: The interval depth with the composite log response of the potential reservoir zones in HT3 well

5.2.4 Well HT4

In Well HT4, two reservoir bodies were delineated including Z1 encountered between 5310.53 and 5321.50 m, while the second Z2, was encountered between 5471.16 and 5475.73 m with gross thicknesses of 42.52 and 38.86 m respectively. Z1 has an average gamma ray of 60 API whereas Z2 has an average gamma ray value of 57 API. Gamma ray histogram for Well HT4 reservoirs depicted considerable points beyond 60 API in Z1, and most points clustering below 60 API in Z2 revealing that Z2 is clean relative to the dirty Z1 in terms of clay content.

Analysis of resistivity log data indicates that the two reservoirs (Z1 and Z2) are hydrocarbon bearing due to their high resistivity responses. Reservoir Z1 is peaking at 767 OHMS with an average 376 OHM of deep resistivity, while reservoir Z2 peaking at 774 OHMS with an average 220 OHMS of deep resistivity.

A cross-plot of the neutron and density logs for Z1 and Z2 reservoirs showed no observable “ballon effect” suggesting the occurrence of oil as the hydrocarbon in Z1 and water in Z2. However, both Z1 and Z2 contain no producible hydrocarbons in Well HT4 (i.e. no pay zone) though with low GR readings and high resistivity readings.

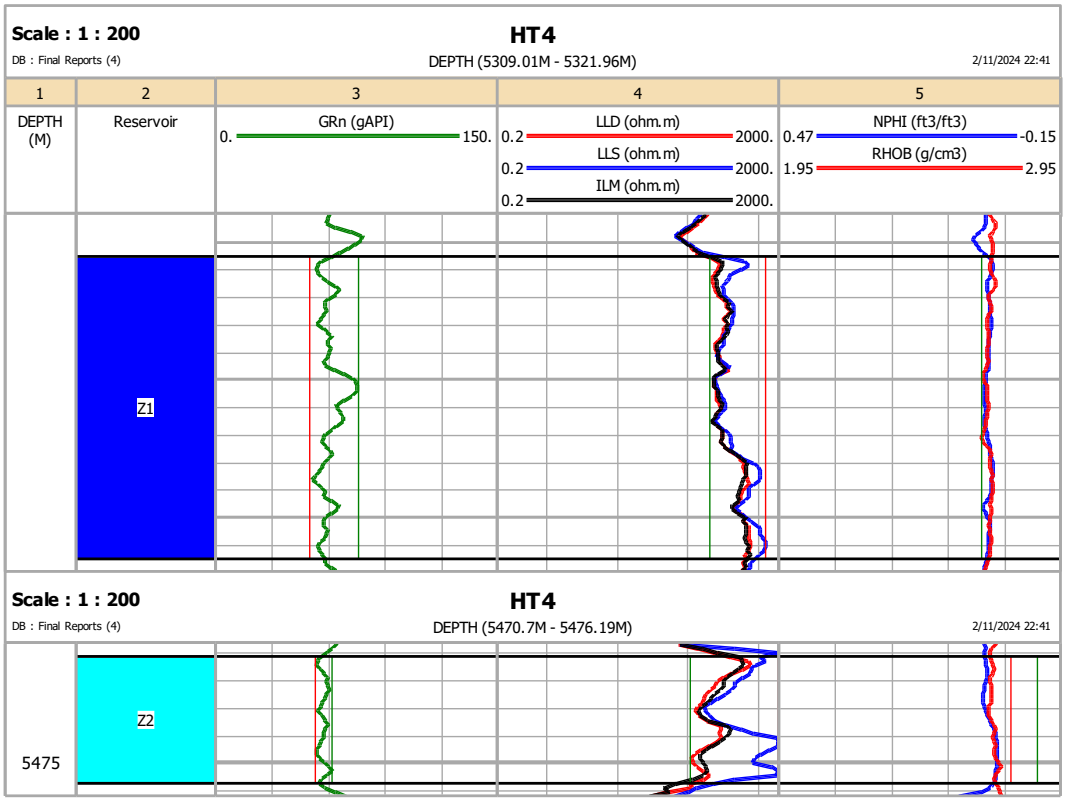

Figure 11: The interval depth with the composite log response of the potential reservoir zones in HT4 well

5.3 Lithology determination

The lithology and mineral composition of the identified reservoir were determined using Neutron-Density, Sonic-Density, M-N lithology and Matrix Identification (MID) crossplots.

5.3.1 Neutron-Density lithology cross plot

Neutron-Density crossplot for the Well HT1 reservoir plotted uneven within all lithological fields indicating heterogeneous lithologies i.e. dolomite, limestone and

sandstone.

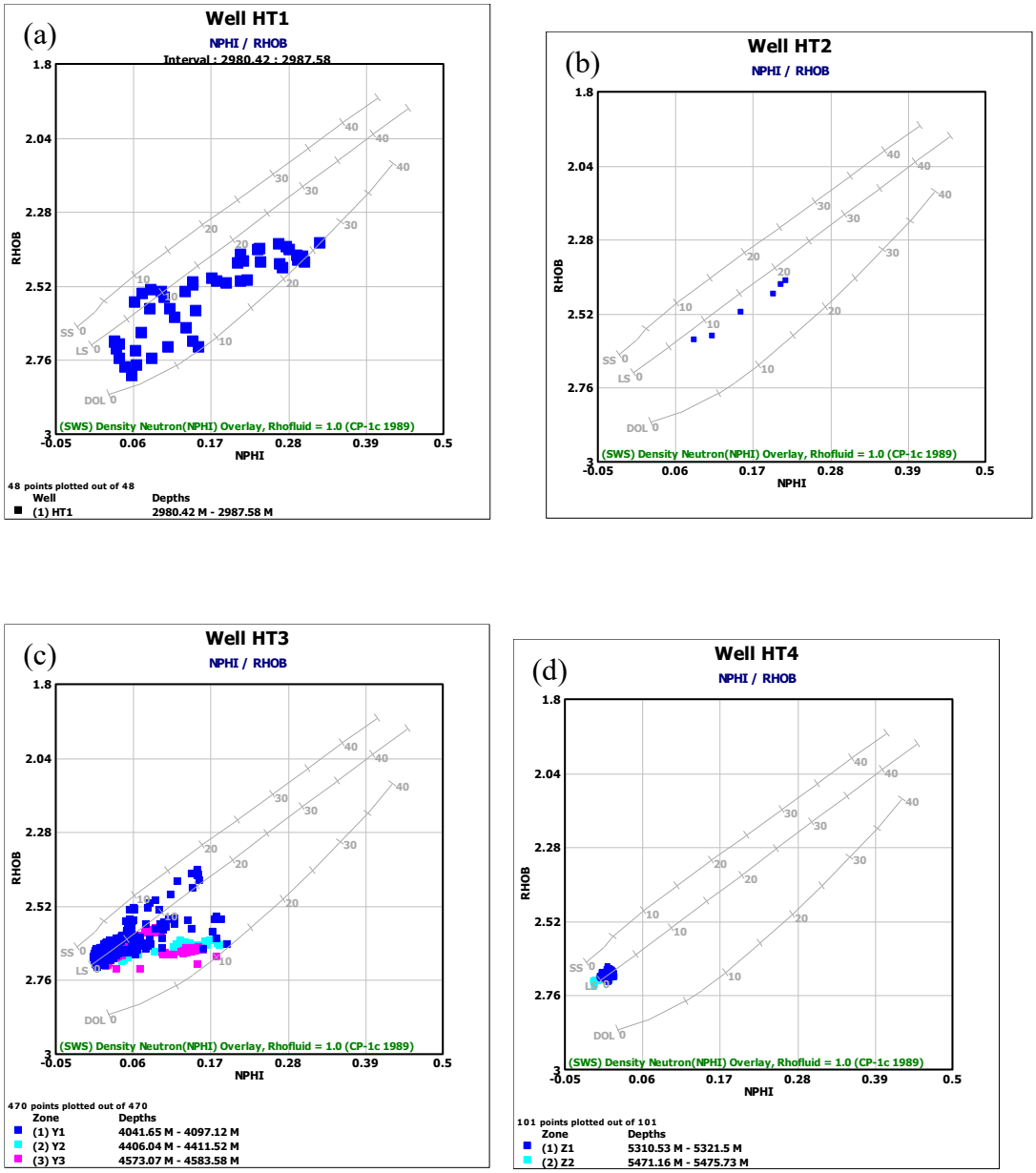

Figure 12: (a) Density-neutron cross-plot of the potential reservoir in Well HT1, (b) Density-neutron cross-plot of the potential reservoir in Well HT2, (c) Density-neutron cross-plot of the potential reservoir in Well HT3, (d) Density-neutron cross-plot of the potential reservoir in Well HT 4.

5.3.2 Sonic-Density cross lithology plot

Figure 13 illustrates sonic-density cross plots depicting reservoir data from Wells HT1, HT2, HT3, and HT4. The data points exhibit irregular scattering across the plots, indicating heterogeneous lithologies comprising dolomite, limestone.

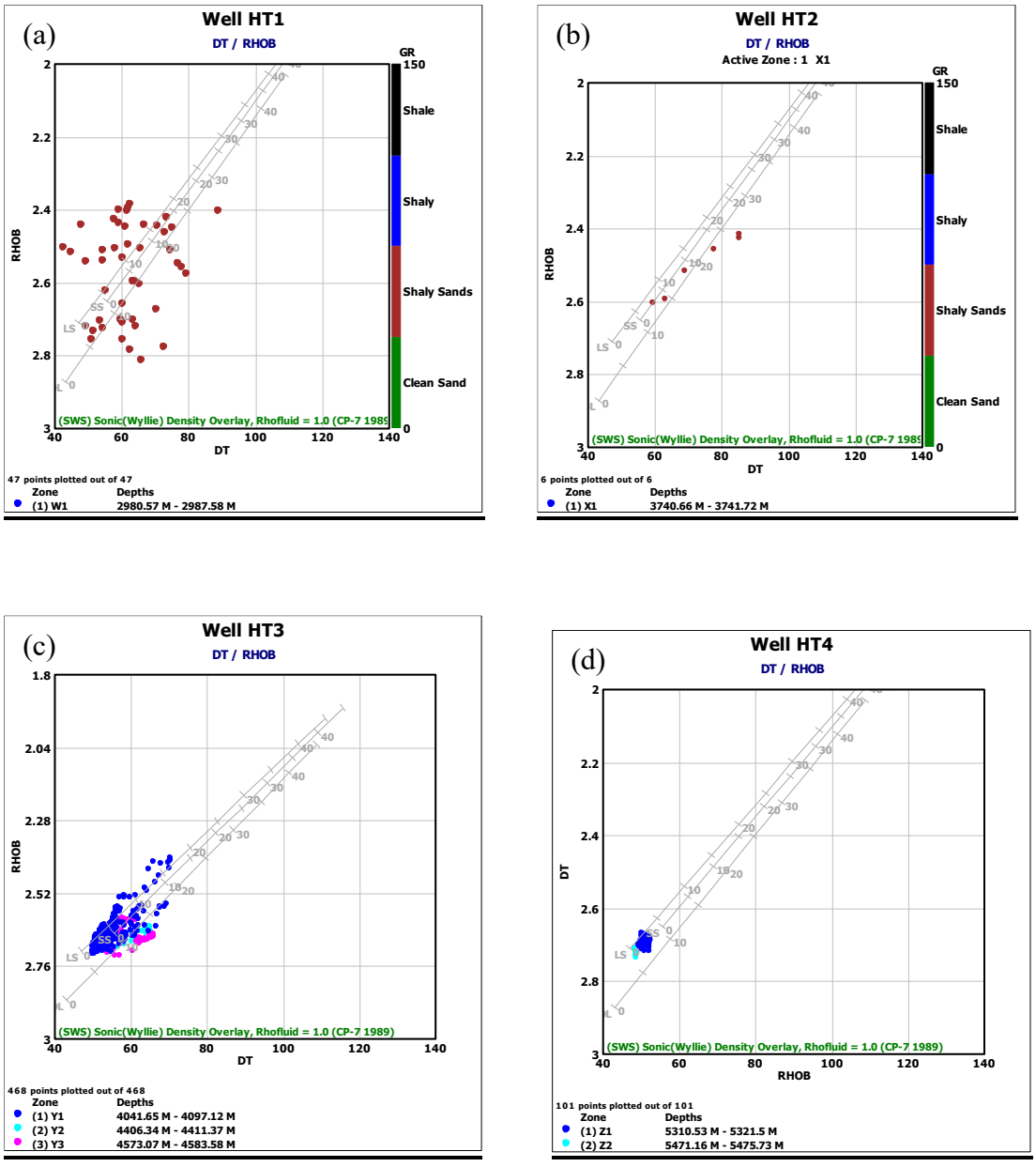

Figure 13: a) Sonic-Density crossplots for Well HT1 and HT4, b) Sonic-Density crossplots for Well HT2, c) Sonic-Density crossplots for Well HT3, d) Sonic-Density crossplots for Well HT4.

5.3.3 M-N lithology cross plot

The M-N lithology plots depict most of the points plotting in the dolomite and calcite with occurrence of secondary porosity in Well HT1 (Figure *17*), indicating that Well HT1 reservoir is chiefly made of calcite matrix with subordinate dolomite and quartz.

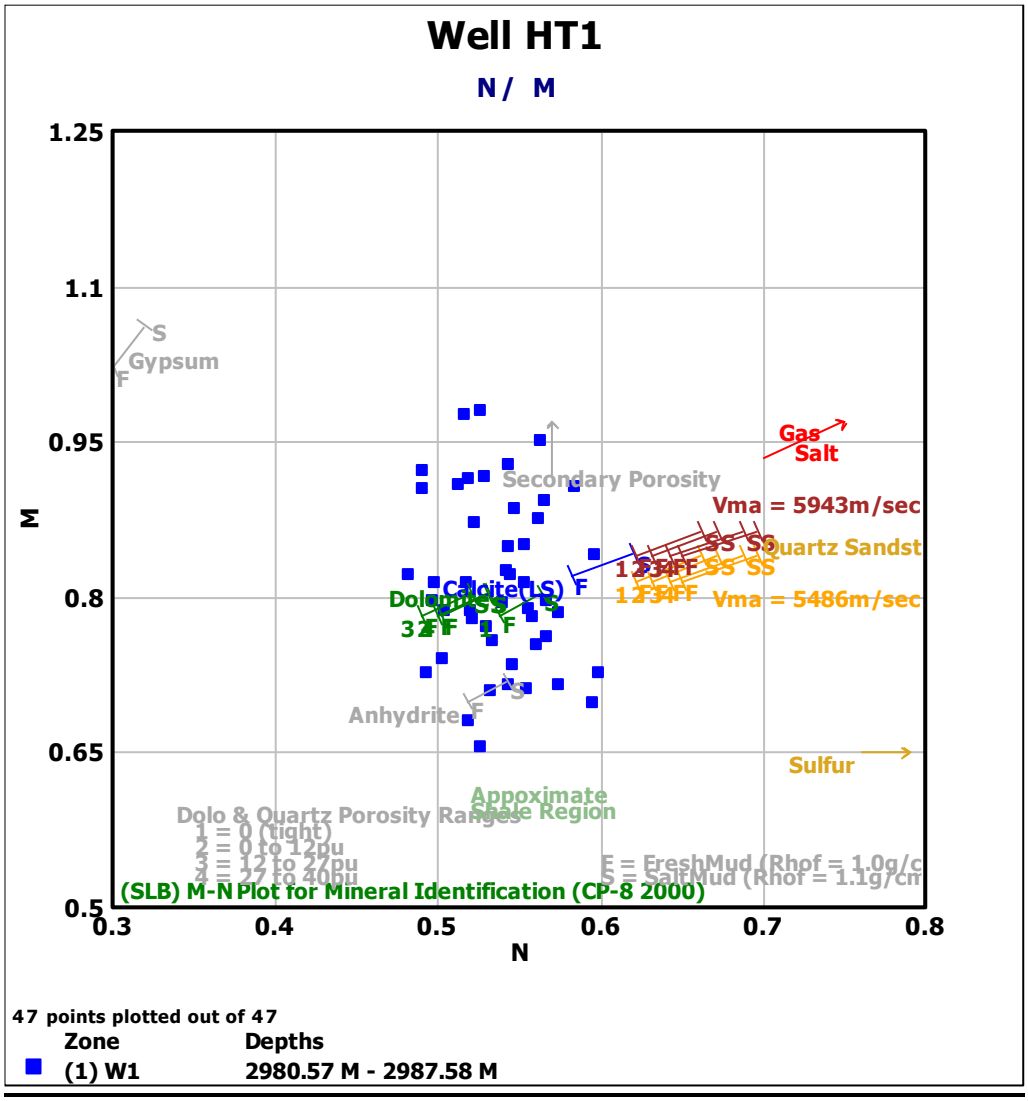

Figure 14: M-N lithology plots for reservoirs in Well HT1.

The M-N lithology plots depict most of the points plotting in the dolomite and calcite

(Figure 15 to Figure 17), indicating that Wells HT2 to HT4 reservoirs are predominantly made of calcite matrix with subordinate dolomite and quartz.

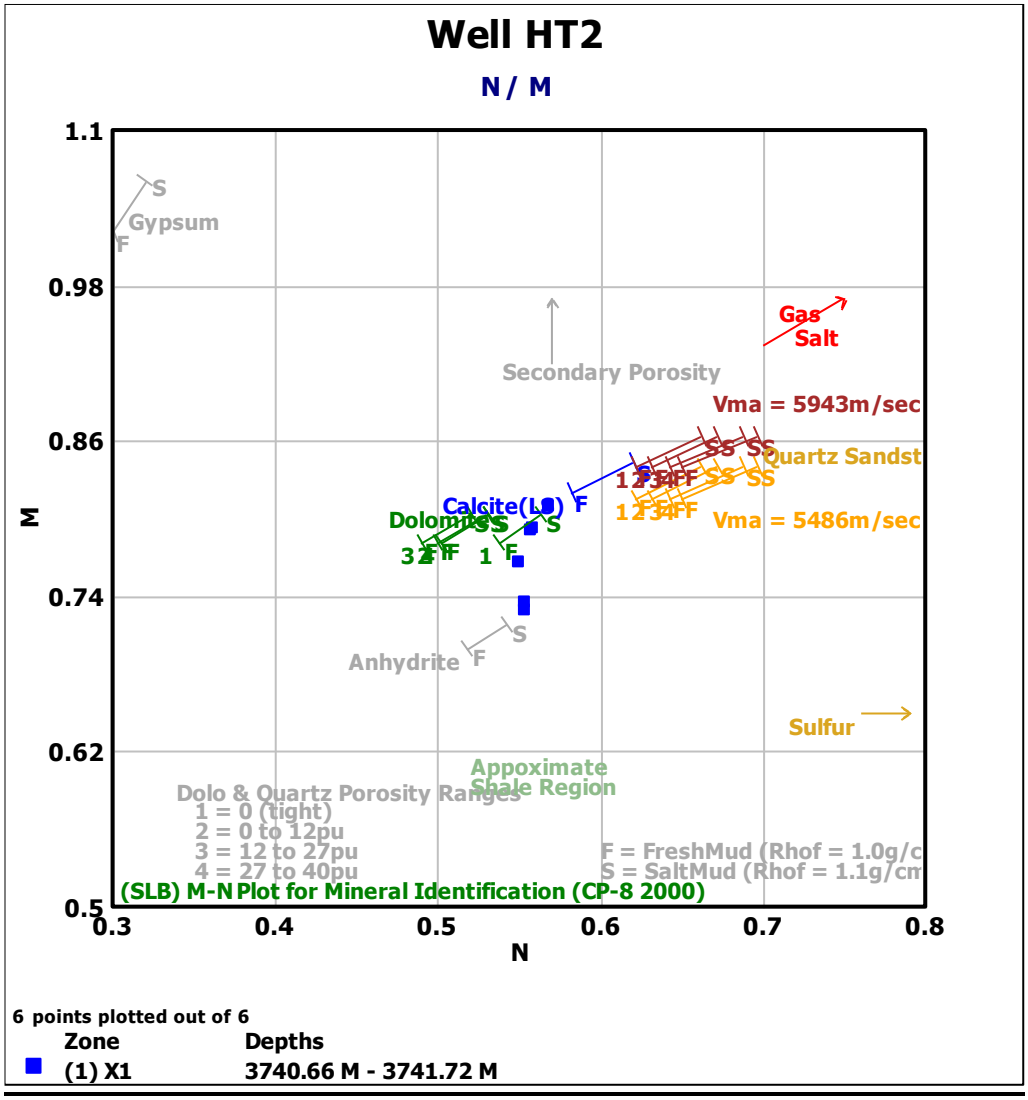

Figure 15: M-N lithology plots for reservoirs in Well HT3

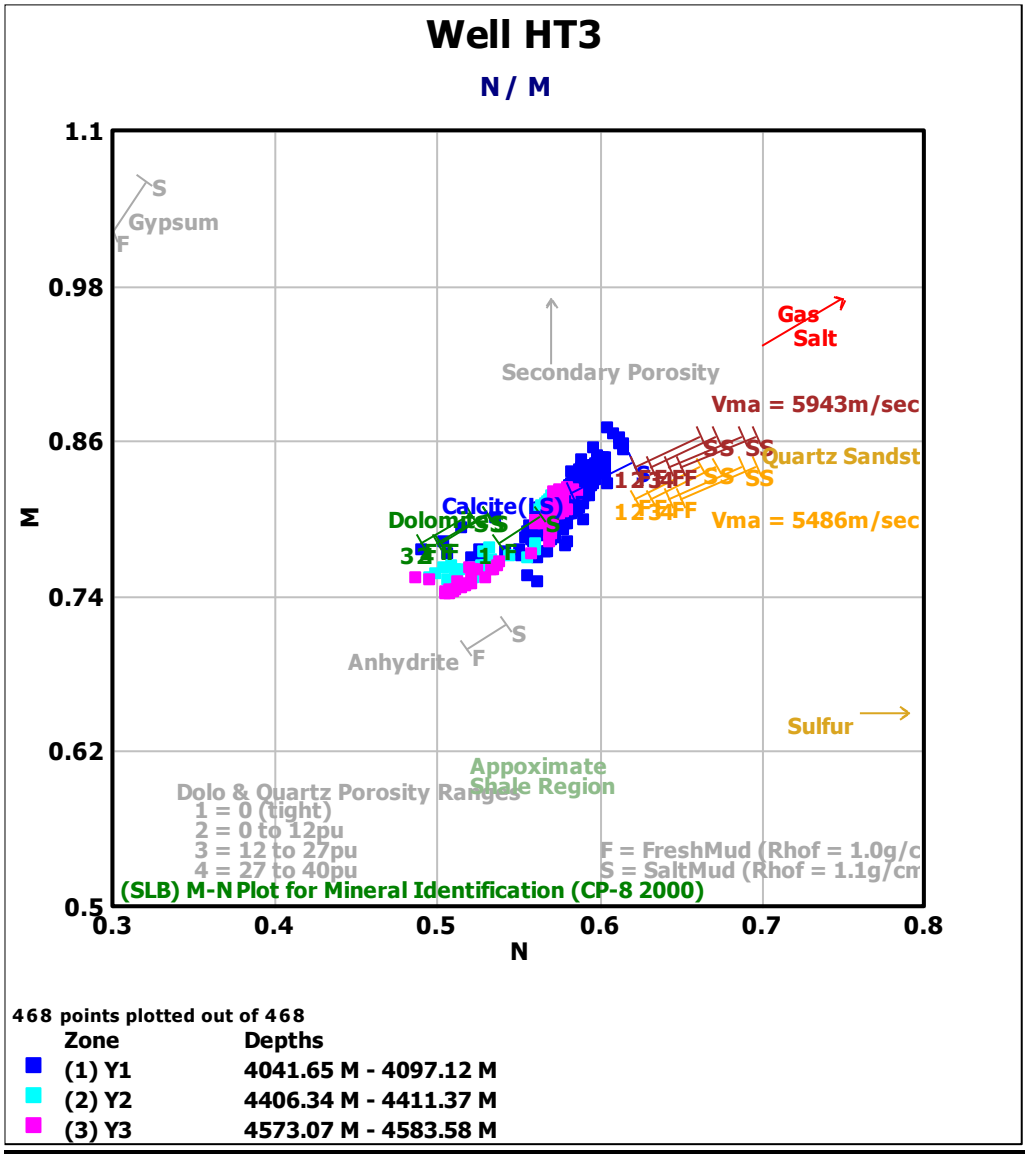

Figure 16: M-N lithology plots for reservoirs in Well HT3

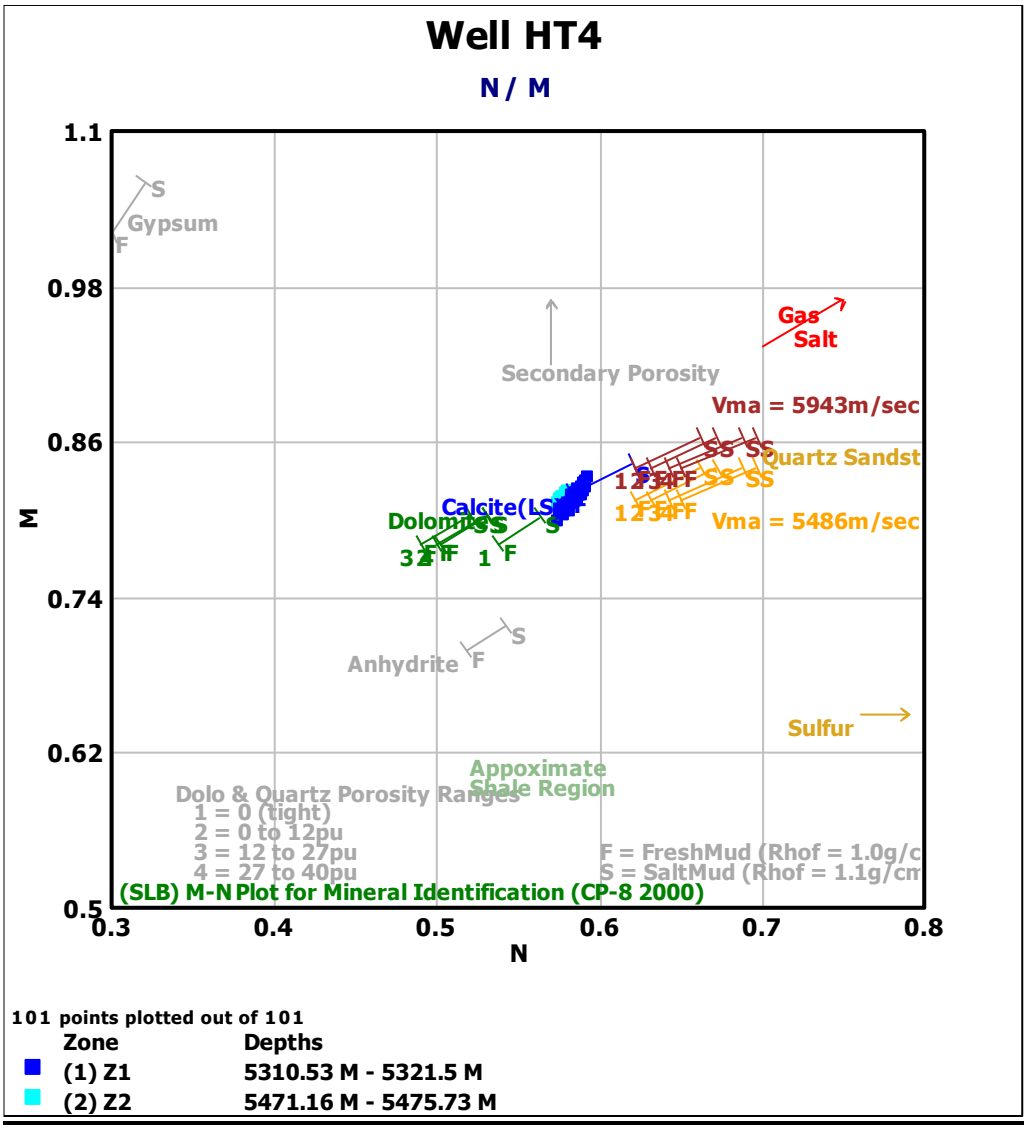

Figure 17: M-N lithology plots for reservoirs in Well HT4

5.3.4 Matrix identification (MID) cross plot

MID lithology plots for show majority of the points clustering around calcite and dolomite field (Figure 18), proving calcite and dolomite as main matrix minerals constituting the reservoir rocks.

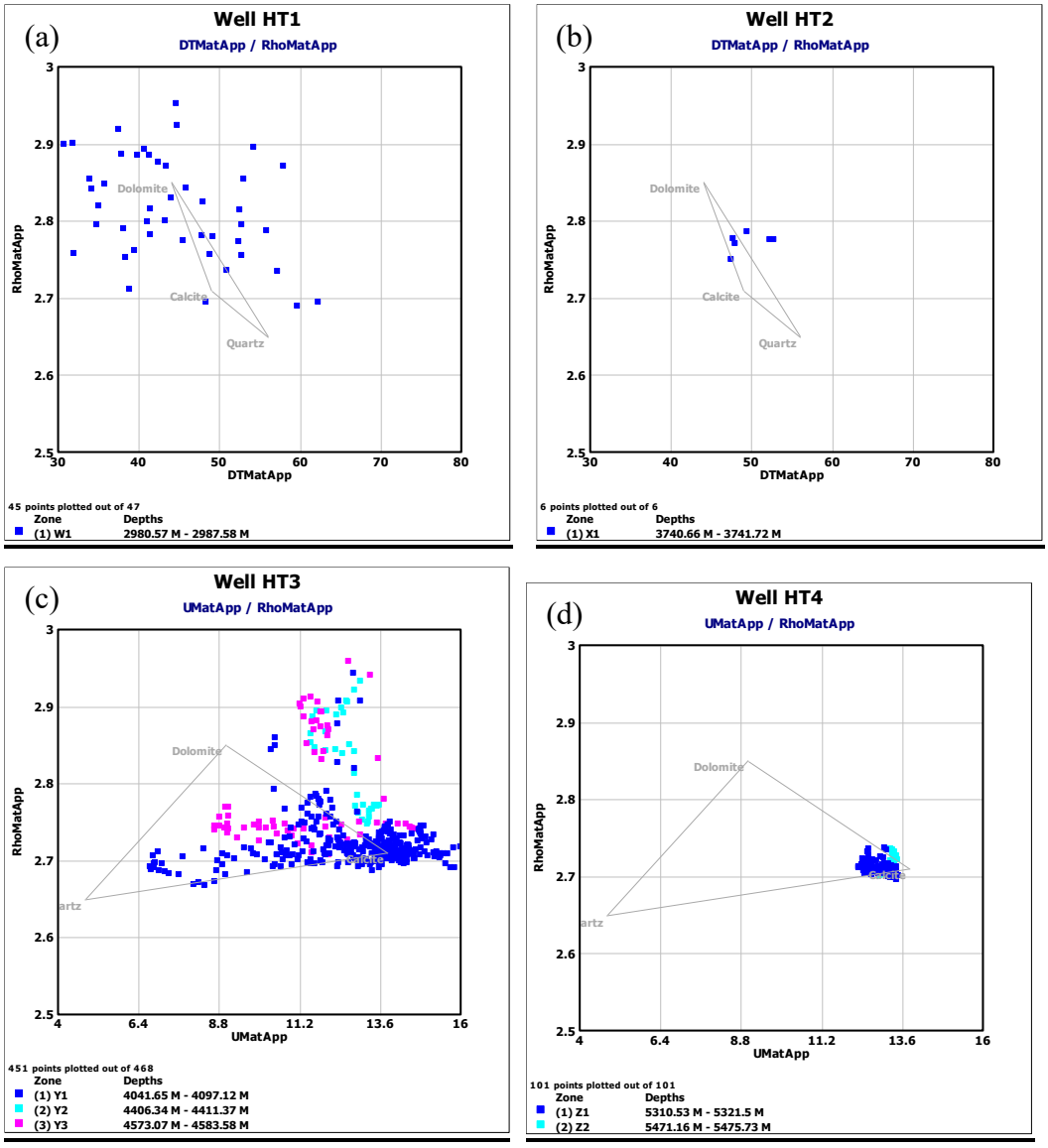

Figure 18: a) MID cross plots for Well HT1 reservoir interval, b)MID cross plots for Well HT2 reservoir interval, c) MID cross plots for Well HT3 reservoir interval, d)MID cross plots for Well HT4 reservoir interval.

5.3.5 THOR-POTA plots for clay

In Well HT1, the Thorium-Potassium plot plotted within the chlorite field, hence chlorite is the dominant clay mineral (Figure *19*). Wells HT2, HT3 and HT4 lacked potassium and thorium logs hence crossplots could not be produced.

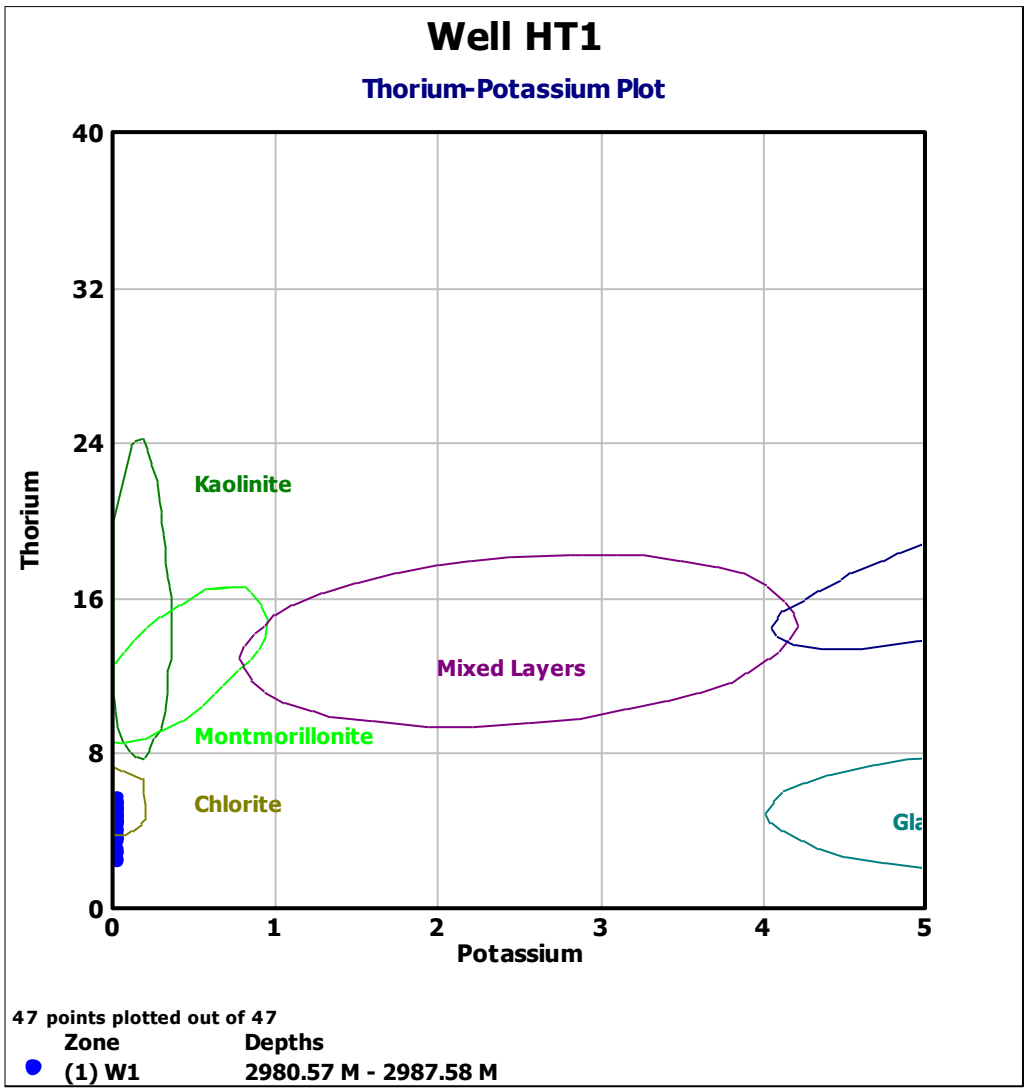

Figure 19: Thorium-Potassium Plot for reservoir W1 in Well HT1

5.4 Clay content, porosity, water saturation and pay zone summary

The clay content, water saturation, porosity values, as well as the pay zones for the various reservoirs were plotted graphically and are presented in showing the reservoir zones (green colour) and the pay zones (red colour) of the delineated reservoir.

5.4.1 Well HT1

One sandstone reservoir was evaluated in well HT1 with a gross thickness of 7.16 m (Table *3*, Figure *20*). This reservoir has very poor reservoir quality and did not yield a properties below detection limit.

Table 3: Summary of calculated reservoir pay parameters for Well HT1

Zone Name	Top (m)	Bottom (m)	Gross (m)	Net (m)	N/G	Av Phi (v/v)	Av Sw (v/v)	Av Vcl (v/v)
W1	2980.57	2987.73	7.16	---	---	---	---	---

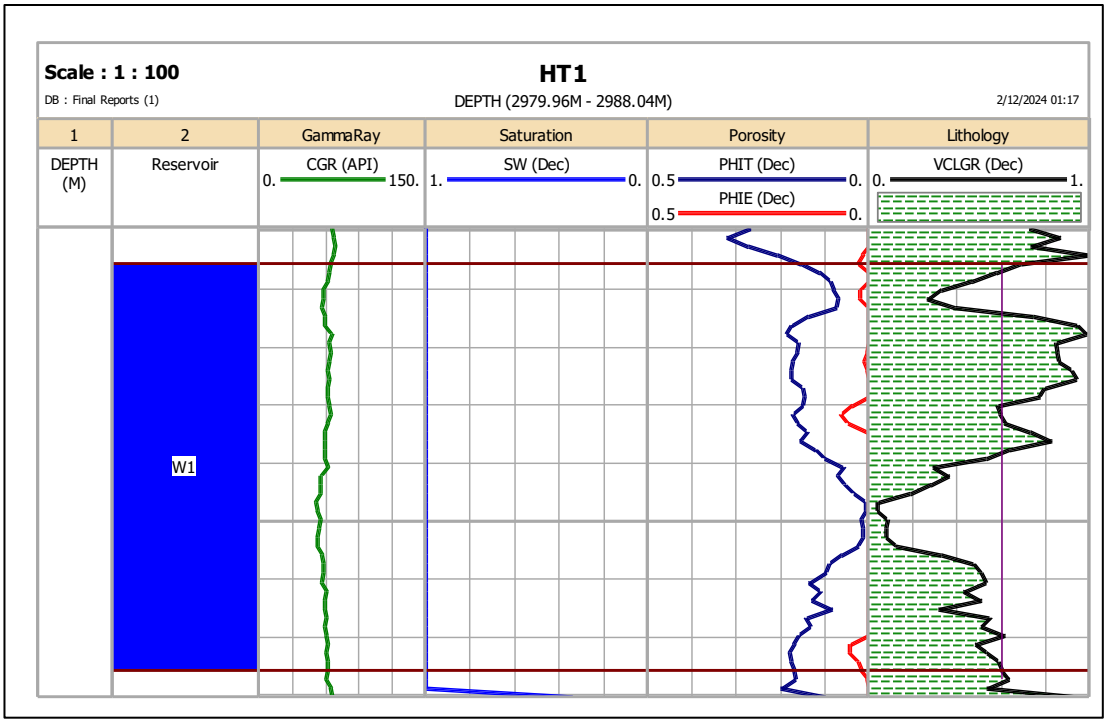

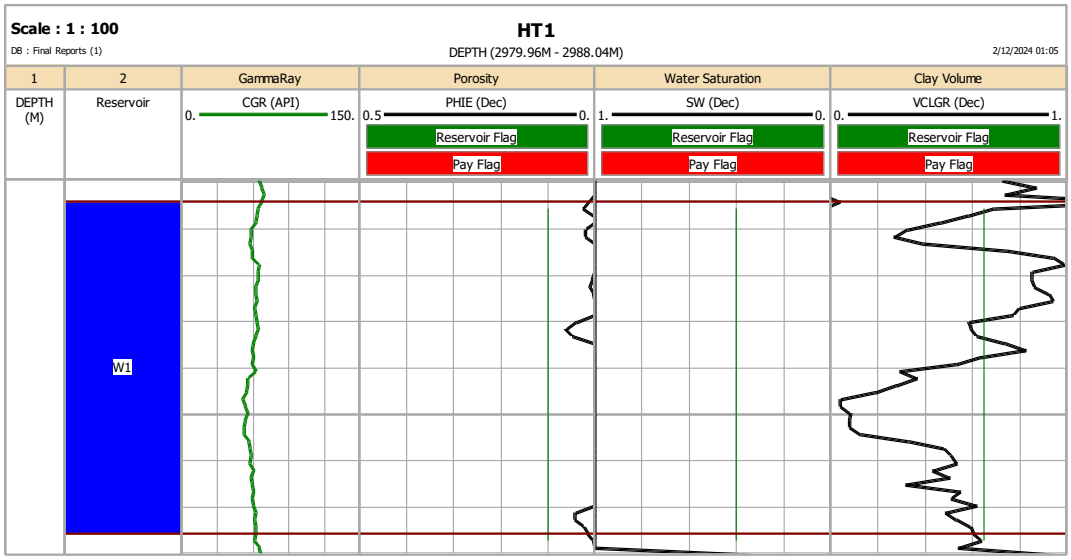

Figure 20: Well HT1 showing the calculated reservoir parameters and pay flags

5.4.2 Well HT2

The clay content, water saturation, porosity values, as well as the pay zones for the various reservoirs were plotted graphically and are presented in showing the reservoir zones (green colour) and the pay zones (red colour) of the X1 reservoir (Figure 21). Petrophysical parameters of all the reservoir zones have been summarized in Table 4. An average porosity of 13.5%, water saturation of 36.1% and volume of clay of 37.7% were calculated as depicted in Table 4 and Figure 21 below.

Table 4: Summary of calculated reservoir pay parameter for well HT2

Zone Name	Top (m)	Bottom (m)	Gross (m)	Net (m)	N/G	Av Phi (v/v)	Av Sw (v/v)	Av Vcl (v/v)
X1	3740.66	3741.72	1.07	0.15	0.143	0.135	0.361	0.377

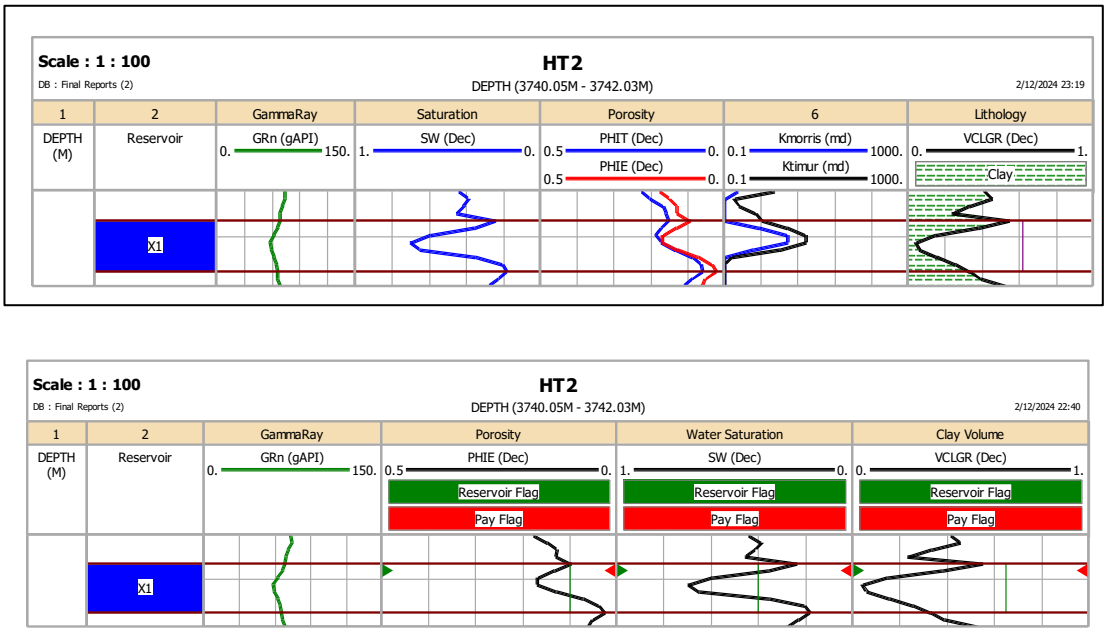

Figure 21: Well HT2 showing calculated reservoir parameters and pay flag

5.4.3 Well HT3

Three reservoirs have been delineated well HT3, total gross thickness of 71.02 m, net thickness of 2.52, average porosity of 12%, water saturation of 61% and volume of clay of 8% were calculated as shown in Table *5* and Figure 22 below.

Table 5: Summary of calculated reservoir pay parameters for well HT3

Zone Name	Top (m)	Bottom (m)	Gross (m)	Net (m)	N/G	Av Phi (v/v)	Av Sw (v/v)	Av Vcl (v/v)
Y1	4041.65	4097.12	55.47	0.76	0.014	0.13	0.54	0.05
Y2	4406.34	4411.37	5.03	1.30	0.258	0.12	0.64	0.08

Y3	4573.07	4583.58	10.52	0.46	0.043	0.10	0.64	0.12
All Zone	4041.65	4583.58	71.02	2.52	0.035	0.12	0.61	0.08

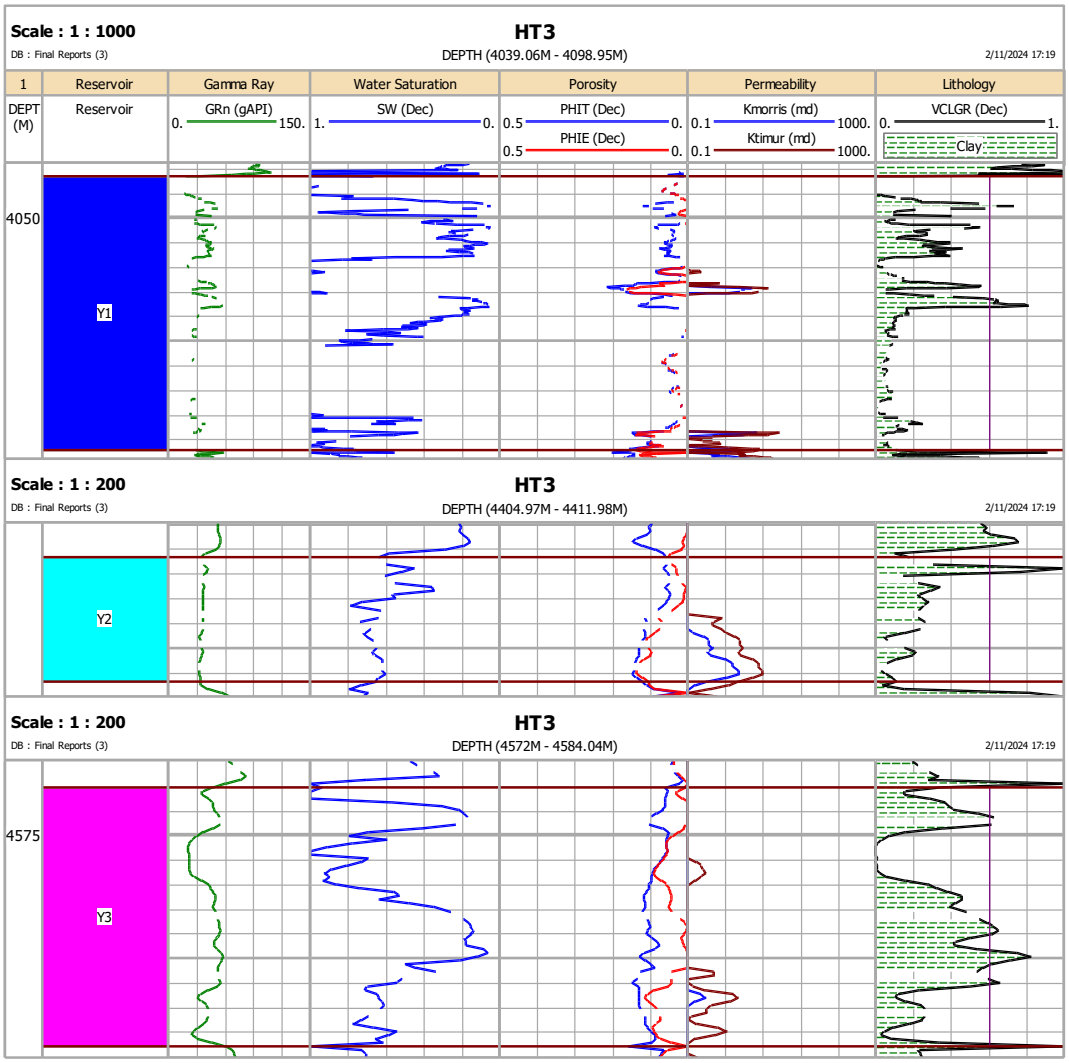

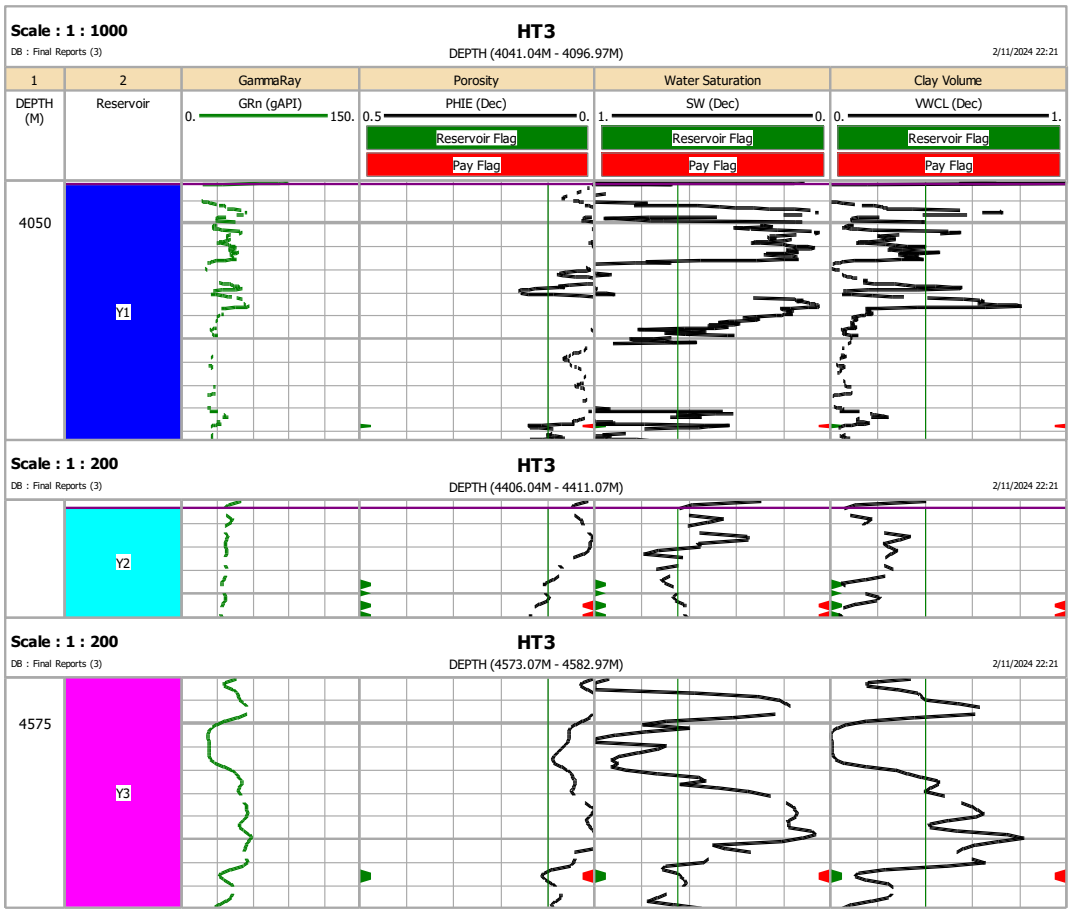

Figure 22: Well HT3 showing calculated reservoir parameters and flags

5.4.4 Well HT4

Two sandstone reservoirs were evaluated in well HT4 with total gross thickness of 81.38 m (Table 6, Figure *23*).

Table 6: Summary of calculated reservoir pay parameters for well HT4

Zone Name	Top (m)	Base (m)	Gross thickness (m)	Net thickness (m)	N/G	Av Vcl (v/v	Av Phi (v/v	Av K (md	AvSw (v/v)

						)	)	)	
Z1	5310.53	5321.50	42.52	---	---	---	---	---	---
Z2	5471.16	5475.73	38.86	---	---	---	---	---	---
All Zones	5310.5	5475.73	81.38	---	---	---	---	---	---

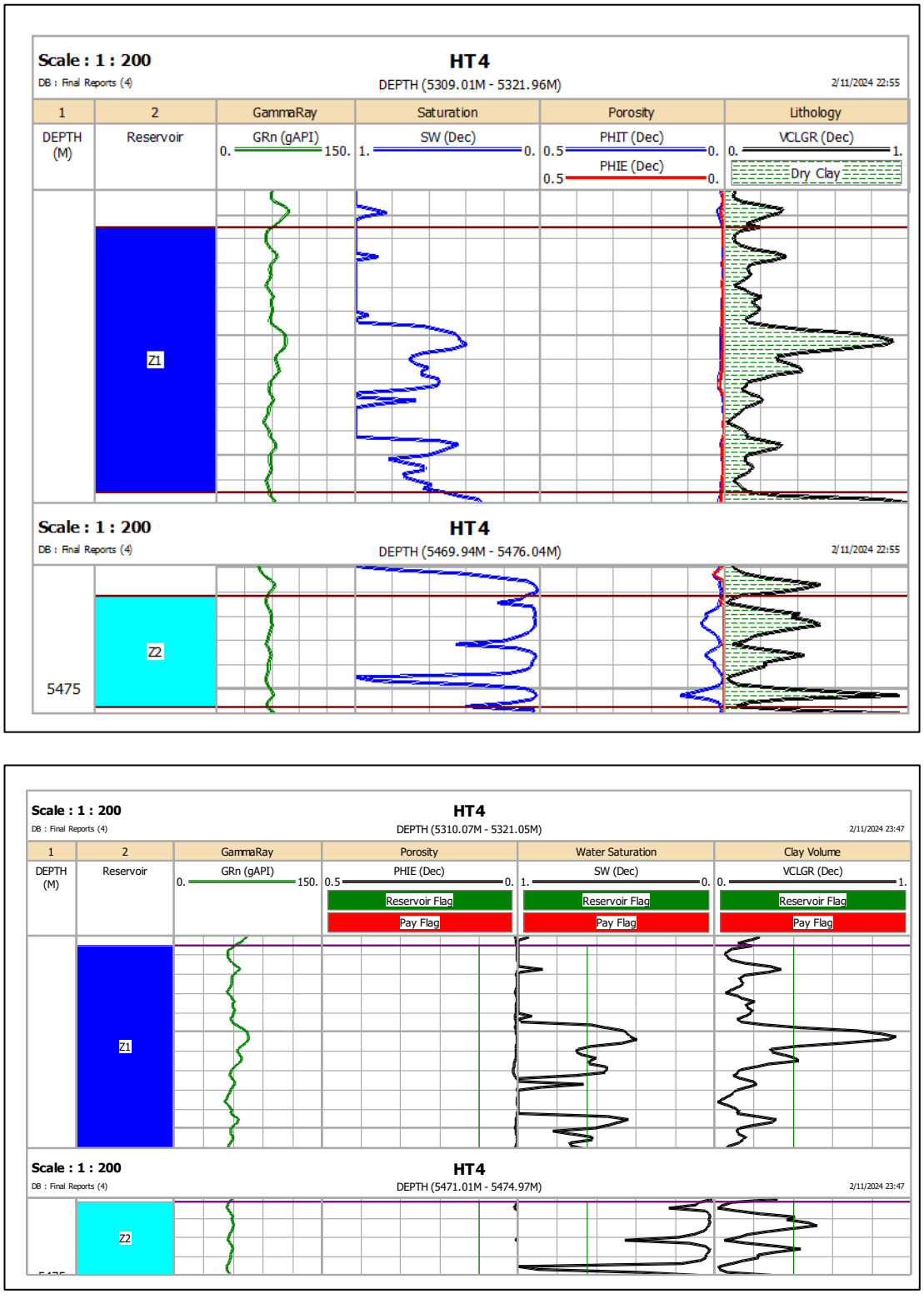

Figure 23: Petrophysical and pay zone summary graphical representation of HT4 reservoir

CHAPTER 6: DISCUSSION

The objective of this research was to interpret the well log data and quantitatively assess the petrophysical properties to identify potential reservoirs for hydrocarbon accumulation. This involved determining the depth and thickness of the zones and discerning the interfaces of oil, gas, or water within the H-T field. The study focused on four exploratory wells: HT1, HT2, HT3, and HT4.

6.1 Identification of Potential Reservoir

Seven reservoir units were identified based on the GR log response of the four wells. In Well HT1, reservoir W1 was identified between 2980.57 m to 2987.73 m with gross thickness of 7.16 m and an average gamma ray response of 60 API. A thin reservoir X1 was delineated from 3740.66 and 3741.72 m in Well HT2, with a gross thickness of only 1.07 m and average gamma ray of 63 API. In Well HT3, three reservoirs' bodies were identified including Y1 encountered between 4041.65 and 4097.12 m, Y2 encountered between 4406.34 and 4411.37 m, while the third Y3 was encountered between 45703.07 and 4583.58 m with gross thicknesses of 55.47 m, 5.03 m and 10.52 m respectively. The average gamma ray values over these reservoir bodies are 30 API, 36 API and 41 API over Y1, Y2, and Y3 respectively. The gamma ray histogram for Well HT3 reservoirs indicated that all points clustering below 60 API revealing that all the reservoirs are clean in terms of clay content. In Well HT4, two reservoir bodies were delineated including reservoir Z1 encountered between 5310.53 and 5321.50 m, while the second reservoir Z2, was encountered between 5471.16 and 5475.73 m with

gross thicknesses of 42.52 and 38.86 m respectively. Z1 has an average gamma ray of 60 API whereas Z2 has an average gamma ray value of 57 API.

6.2 Quantification of fluid in the Reservoir

Analysis of HT4 resistivity log data indicates that Z1 and Z2 reservoirs are hydrocarbon bearing because of their high resistivity responses. Reservoir Z1 is peaking at 767 OHMS with an average 376 OHM of deep resistivity, while reservoir Z2 peaking at 774 OHMS with an average 220 OHMS of deep resistivity. A cross-plot of the neutron and density logs for Z1 and Z2 reservoirs showed no observable "balloon effect" signifying the occurrence of oil as the hydrocarbon. However, both Z1 and Z2 contain no producible hydrocarbons (no pay zone) despite having low GR readings and high resistivity readings. This is a characteristic of calcareous interbeds which depicts unique features of natural gamma less than 80 API and higher lateral resistivity than any other sandstone (Zhu et al., 2018).

The study delineated four main reservoirs (X1 in Well HT2, and Y1, Y2, and Y3 in Well HT3), although all water-bearing reservoirs.

6.3 Petrophysical Evaluation

Well log dataset from four wells drilled in the H-T field were used to conduct detailed petrophysical analysis and reservoir characterization of the study area. The four main reservoirs delineated in the study area are lithologically heterogeneous composed of

very fine grains of calcite, dolomite, and quartz.

Petrophysical analysis carried out on the well log dataset indicate reservoirs that are discontinuous within the same well and when compared to other wells. Some of the delineated reservoirs are thin and could resemble a thin stratigraphic sand beds which thin out and deposited either as channel sands or as short turbiditic events (Chongwain et al., 2019).

Reservoir X1 in Well HT2 has an estimated average porosity of 13.5%, water saturation of 36.1% and volume of clay of 37.7%. In Well HT3, across the three main reservoir zones Y1, Y2 and Y3, a total gross thickness of 71.02 m, net thickness of 2.52 m, average porosity of 12%, and water saturation of 61% and volume of clay of 8% was estimated. This average porosity is quite consistent with wells which are close to the H-T Field. The nearer wells have a 45m to 50m of net in the reservoir interval with 12% to 14% porosity (Chandler et al., 2018). Wells with very little net are not uncommon in the Walvis Basin, e.g. the Wingat-1 well has 0.46 m of net in the reservoir interval (Chandler et al., 2018).

The results of average volume of shale indicate that 0.08 v/v was calculated for Well HT3. According to Hilchie (1978), the volume of shale value for HT3 is within the limiting value of 0.15 v/v for a very good reservoir, thus will not affect the reservoir effective porosity negatively (Okeugo et al., 2021). In Well HT2, the average volume

of shale was calculated as 0.38 v/v which is more than double the limiting value of 0.15 v/v. this suggest that reservoir X1, with Vsh value of 0.38 v/v decimal is above the limit of (>10% - 15%) which could affect the value of water saturation value. Observation shows that there is no significant variation in average porosity and effective porosity values in Wells HT2 and HT3, as both wells are in the same fault block and no change in depositional environment caused by faulting activities (Okeugo et al., 2021).

The identification of reservoir quality is key objective in reservoirs characterization process, the quality of a reservoir is defined by its hydrocarbon storage capacity, and storage capacity (Al-Jawad & Saleh, 2019). The reservoir capacity is determined by porosity, while deliverability is determined by permeability. Therefore, the primary variables influencing reservoir quality are permeability and porosity (El Sharawy & Nabawy, 2019).

According to Hartmann and MacMillan (1992), water distribution in the reservoir depends on the height above the free water level, pore type, and hydrocarbon type.

According to Intawong et al., (2017), the Murombe well in the Walvis Basin had encountered water wet reservoir with a 242 m gross section, 15% net to gross ratio and average porosity of 19%. Holtar & Forsberg (2000) ascribe a very good reservoir quality with up to 25% porosity in Well 1911/15-1 in the northern Walvis Basin. This

shows that Late Cretaceous turbidities in the Walvis Basin are having high quality reservoir sands.

Determination of the lithology of H-T field using four types of cross plots, proved that the lithology consisted chiefly of limestone. The MID and M-N cross plots proved calcite as the primary mineral composition and dolomite the secondary mineral.

The Thorium-Potassium plot exhibited clustering within the chlorite field, suggesting chlorite as the predominant clay mineral present. Clay minerals are typically considered detrimental to sandstone reservoir quality due to their ability to obstruct pore throats, with their presence on grain surfaces in the form of films, plates, and bridges (Jiang, 2012). Furthermore, certain clay minerals contribute to chemical compaction and significantly accelerate porosity loss rates in limestone reservoirs (Brown, 1997). The formation of chlorite can be attributed to either primary deposition preceding sediment formation or secondary diagenetic events occurring subsequent to sediment formation (Chongwain et al., 2019).

Reservoir properties such as porosity, permeability, and saturation can highlight the specific features such as fractures and vugs of carbonates (Stadtműller & Jarzyna, 2023; Kargarpour, 2020). Better understanding of reservoir characterization is essential to field development planning success, and precise reservoir characterization is a requirement for more effective and better management of heterogeneous (Shedid,

2018).

Reservoir presence in H-T Field is a concern as some wells have either failed to encounter the reservoir or, when they have, it has been thinner than expected or tight (for example, the HT2 well). However, HT3 well have encountered a reasonable thickness of reservoir with reasonable quality. These results suggest that the reservoir presence and effectiveness can be variable.

Hydrocarbon reservoirs seem to be absent in the H-T Field, but all major elements of a valid hydrocarbon system are present in the Walvis Basin (Intawong et al., 2017), which makes further evaluation and exploration worthwhile. The findings from this study have implication on a having a comprehensive understanding of the petroleum system in the Walvis Basin. It may likewise serve as an analogue for similar reservoirs elsewhere along petroliferous margins.

CHAPTER 7: CONCLUSION AND RECOMMENDATIONS

The petrophysical analyses conducted in this study indicate that the reservoir sand units within the H-T Field predominantly contain water. The analysis reveals a very fine grain size; however, the petrophysical properties of this reservoir are not conducive to hydrocarbon accumulation, preservation, and generation.

Mineral identification cross-plots revealed that the reservoirs are lithologically heterogeneous, composed of very fine grains of calcite, dolomite, and quartz. This study additionally identified the existence of calcareous interlayers, interpreted as calcareous tight reservoirs within the H-T field, exemplified by reservoirs W1, Z1, and Z2.

The findings from this study have implication on a having a comprehensive understanding of the petroleum system in the Walvis Basin. It may likewise serve as an analogue for similar reservoirs elsewhere along petroliferous margins.

Further calibration of the log analysis parameters with core data is strongly recommended to validate the calculated values, particularly since the permeabilities for the reservoir sand units remain uncharacterized.

Flow zone characterization should be carried out. Flow zones are required for identifying, describing, and quality ranking flow units include lithological,

petrographic, and petrophysical data. Also, seismic dataset can be analyzed to understand if there are any tectonostratigraphic control.

REFERENCES

Afizu, M. (2013). Determining the Relationship between Resistivity, Water and Hydrocarbon Saturation of Rock Formation Using Composite Well Logs. Academic Journal of Interdisciplinary Studies, 2(13), 119–124. https://doi.org/10.5901/ajis.2013.v2n13p119

Al-Jawad, S.N. & Saleh, A.H. (2020). Flow units and rock type for reservoir characterization in carbonatreservoir: case study, south of Iraq. Journal of Petroleum Exploration and Production Technology, 10(1), 1-20.

Amigun, J. O., & Odole, O. A. (2013). Petrophysical Properties Evaluation for Reservoir Characterisation of SEYI Oil Field (Niger-Delta). International Journal of Innovation and Applied Studies, 3(3), 765–773.

Asquith, G., & Krygowski, D. (2004). AAPG Methods in Exploration, No. 16, Chapter 2: Spontaneous Potential.

Baban, D. H., Abdulla, A. S., & Omar, H. M. (2018). Applications of quick look methods for evaluating the Middle Miocene Jeribe Formation from a selected well in Jambour Oilfield, Kurdistan Region, northern Iraq. *Journal of Petroleum Exploration and Production Technology*, *8*, 733-741.

Baby, G., Guillocheau, F., Morin, J., Ressouche, J., Robin, C., Broucke, O., & Dall'Asta, M. (2018). Post-rift stratigraphic evolution of the Atlantic margin of Namibia and South Africa: Implications for the vertical movements of the margin and the uplift history of the South African Plateau. *Marine and Petroleum Geology*, *97*, 169-191.

Bray, R., Lawrence, S., & Swart, R. (1998). Source rock, maturity data indicate potential off Namibia. *Oil and Gas Journal*, *96*(32).

Brink, L. (2018). *Geological Well Completion Report of Well CORMORANT-1 PEL 37 Walvis Basin Offshore Namibia*. Internal Tullow Oil report. Unpublished.

Brown, A. (1997). Porosity variation in carbonates as a function of depth: Mississippian Madison Group, Williston Basin.

Chandler, P., Mullinor, J., Rao, A., & Smidt-Olsen, B. (2018). Competent Person's Report on exploration prospects in Licence 0029, offshore Namibia, for Global Petroleum Limited.Unpublished.

Crain, E.R. (2016). Visual rule for water saturation, petrophysical handout. Retrieved March 16, 2024. https://www.spec2000.net/

Cole, G.A. (2021). Orange Basin Petroleum Geochemistry and 3D Modeling 2021: unpublished paper. ResearchGate, DOI: 10.13140/RG.2.2.23315.20000.

Chongwain, G. M., Osinowo, O. O., Ntamak-Nida, M. J., Biouele, S. E. A., & Nkoa, E. N. (2019). Petrophysical characterisation of reservoir intervals in well-X and well-Y, M-Field, offshore Douala Sub-Basin, Cameroon. Journal of Petroleum Exploration and Production Technology, 9(2), 911–925. https://doi.org/10.1007/s13202-018-0562-0

Chongwain, G. C., Osinowo, O. O., Ntamak-Nida, M. J., & Nkwanyang, T. L. (2019). Lithological typing, depositional environment, and reservoir quality characterization of the "M-Field," offshore Douala Basin, Cameroon. *Journal of Petroleum Exploration and Production Technology*, *9*, 1705-1721.

Clemson, J., Cartwright, J., & Booth, J. (1997). Structural segmentation and the influence of basement structure on the Namibian passive margin. *Journal of the Geological Society*, *154*(3), 477-482.

Das, B., & Chatterjee, R. (2018). Well log data analysis for lithology and fluid identification in Krishna-Godavari Basin, India. Arabian Journal of Geosciences 2018 11:10, 11(10), 1–12. https://doi.org/10.1007/S12517-018-3587-2

Dauteuil, O., Rouby, D., Braun, J., Guillocheau, F., & Deschamps, F. (2013). Post-breakup evolution of the Namibian margin: Constraints from numerical modeling. *Tectonophysics*, *604*, 122-138.

De Vera, J., Granado, P., & McClay, K. (2010). Structural evolution of the Orange Basin gravity-driven system, offshore Namibia. *Marine and Petroleum Geology*, *27*(1), 223-237.

Domingos, K. M. (2018). *Well log petrophysics and re-interpretation of the exploration target intervals in the southern Walvis basin* (MSc dissertation, University of Namibia). Retrieved on May 25, 2022 from https://repository.unam.edu.na/items/2613a478-739c-4a63-832b-0ecaef4ed1dc

Ellis, D. V., & Singer, J. M. (2007). *Well logging for earth scientists* (Vol. 692). Dordrecht: Springer.

El Sharawy, M.S., & Nabawy, B.S. (2019). Integration of electrofacies and hydraulic flow units to delineate reservoir quality in uncored reservoirs: a case study, Nubia Sandstone Reservoir, Gulf of Suez, Egypt. Natural Resources Res 1:2. https ://doi.org/10.1007/s11053-018-9447-7

Galp Energia. (2013). Wingat-1 exploration well results. Retrieved March 07, 2024, from https://www.galp.com/corp/en/investors/publications-and-announcements/investor-announcements/investor-announcement/id/397/wingat-1-exploration-well-results

Garzanti, E., Vermeesch, P., Andò, S., Lustrino, M., Padoan, M., & Vezzoli, G. (2014). Ultra-long distance littoral transport of Orange sand and provenance of the Skeleton Coast Erg (Namibia). *Marine Geology*, *357*, 25-36.

Hartmann, D.J., & MacMillan, L. (1992). Petrophysics of the Wasatch Formation Mesa Verde Group, Natural Buttes Producing Area Unita Basin, Utah. Utah Geological Association.

Hedley, R., Intawong, A., Winter, F., & Sibeya, V. (2022). Hydrocarbon play concepts in the Orange Basin in light of the Venus and Graff oil discoveries. *First Break*, *40*(5), 91-95.

Helander, D. P. (1983). Fundamentals of formation evaluation

Hilchie, D.W. (1978). Applied openhole Log interpretation. Hilchie Inc, Golden, Colrado, D.W.

History. (2022, May 25). Retrieved from https://www.namcor.com.na/history/#1668071916357-43234fab-4aef

Hodgson, N., & Intawong, A. (2013). Derisking deep-water Namibia. First Break, 31(12), 91–96. https://doi.org/10.3997/1365-2397.31.12.72256

Holtar, E. & Forsberg, A.W. (2000). Postrift development of the Walvis basin, Namibia, Results from the exploration campaign in Quadrant 1911. – In: MELLO, M .R. & KATZ, B.J. (eds.): Petroleum Systems of South Atlantic margins. – AAPG Memoir, 73, 429-446.

Intawong, A., Hodgson, N., Rodriguez K., & Sibeya V. (2017). Hunting turbidites in the Walvis Basin, offshore Namibia. September 2.

Jiang, S. (2012). Clay minerals from perspective of oil and gas exploration. Clay minerals in nature-their characterization, modification and application, 21-38.

Kargarpour, M. A. (2020). Carbonate reservoir characterization: an integrated approach. Journal of Petroleum Exploration and Production Technology, 10(7), 2655-2667.

Katz, A. J., and A. H. Thompson. "Quantitative prediction of permeability in porous rock." *Physical review B* 34.11 (1986): 8179.

Kukulus, M. (2004). A quantitative approach to the evolution of the central Walvis Basin offshore NW-Namibia: structure, mass balancing, and hydrocarbon potential [Unpublished Doctoral dissertation] University of Würzburg. Retrieved on May 25, 2022, from http://eprints.uanl.mx/5481/1/1020149995.PDF

Lenciono, L.C. (2016). Resource report for certain assets in offshore Namibia and report for assets in offshore Guyana, Prepared according to national Instrument 51-101. Internal report (Eco Atlantic (PTY) Ltd). Unpublished.

Light, M. P. R., Maslanyj, M. P., Greenwood, R. J., & Banks, N. L. (1993). Seismic sequence stratigraphy and tectonics offshore Namibia. *Geological Society, London, Special Publications*, *71*(1), 163-191.

Lyaka, Aneth. L., & Mulino, Gabriel. D. (2018). Petrophysical Analysis of the Mpapai Well Logs in the East Pande Exploration Block, Southern Coast of Tanzania: Geological Implication on the Hydrocarbon Potential. Open Journal of Geology, 8(8), 781–802. https://doi.org/10.4236/ojg.2018.88046

Magoon, L. B., & Dow, W. G. (1994). The petroleum system: chapter 1: Part I. Introduction.

McDermott, K., Gillbard, E., & Clarke, N. (2015). From Basalt to Skeletons–the 200-million-year history of the Namibian margin uncovered by new seismic data. First Break, 33(12).

Mello, M. R. (2022, November). Offshore Namibia: The sleeping giant deep-water hydrocarbon frontier has awakened. In *SEG International Exposition and Annual Meeting* (p. D011S058R003). SEG.

Mello, M. R., De Azambuja Filho, N. C., Bender, A. A., Barbanti, S. M., Mohriak, W., Schmitt, P., & De Jesus, C. L. C. (2012). The namibian and brazilian southern south atlantic petroleum systems: Are they comparable analogues? Geological Society Special Publication, 369(1), 249–266. https://doi.org/10.1144/SP369.18

Nkwanyang, L. T., Ehinola, O. A., Takem, J. E., Nguema, P., Makoube, S. E., & Chongwain, G. M. (2018). Depositional setting and petrophysical evaluation of reservoir of the K-field in the Western offshore Depobelt, Rio Del Rey basin, Cameroon. *International Journal of Geosciences*, *9*(9), 528-546.

Nwankwo, C., Anyanwu, J., & Ugwu, S. (2014). Integration of seismic and well log data for 17 petrophysical modeling of sandstone hydrocarbon reservoir in Niger Delta. Scientia Africana, 13(1), 186–199.

Okeugo, C. G., Onuoha, K. M., & Ekwe, A. C. (2021). Lithology and fluid discrimination using rock physics-based modified upper Hashin–Shtrikman bound: an example from onshore Niger Delta Basin. Journal of Petroleum Exploration and Production, 11(2), 569-578.

Opuwari, M. (2010). *Petrophysical evaluation of the Albian age gas bearing sandstone reservoirs of the OM field, Orange basin, South Africa* (Doctoral dissertation, University of the Western Cape).

Petroleum Agency South Africa. (n.d.). Petroleum Exploration Potential of the Orange Basin [Brochure]. https://www.petroleumagencysa.com/images/pdfs/Orange_Basin_Brochure-JS-02-18w1.pdf

Poupon, A., & Leveaux, J. A. C. Q. U. E. S. (1971, May). Evaluation of water saturation in shaly formations. In *SPWLA Annual Logging Symposium* (pp. SPWLA-1971). SPWLA.

Rider, M. H. (1986). The geological interpretation of well logs.

Rider, M. (2002). The Geological Interpretation of Well Logs. Rider-French Consulting Ltd.

Rider, M.H. & Kennedy, M. (2011). *The geological interpretation of well logs* (3rd ed.). Rider-French Consulting Ltd.

Roger, M.S.L.A.T.T. (2006) Stratigraphic reservoir characterization for petroleum geologists, geophysicists, and engineers. Handbook of petroleum exploration and production, vol 6. Elsevier, Amsterdam

Sam-Marcus, J., Enaworu, E., Rotimi, O. J., & Seteyeobot, I. (2018). A proposed solution to the determination of water saturation: using a modelled equation. *Journal of Petroleum Exploration and Production Technology*, *8*, 1009-1015.

Schmidt, S. (2004). The petroleum potential of the passive continental margin of South-Western Africa–a basin modelling study. *Unpublished PhD dissertation, Fakultät für Georessourcen und Materialtechnik der Rheinisch-Westfälischen Technischen Hochschule Aachen, Germany*.

Senosy, A. H., Ewida, H. F., Soliman, H. A., & Ebraheem, M. O. (2020). Petrophysical analysis of well logs data for identification and characterization of the main reservoir of Al Baraka Oil Field, Komombo Basin, Upper Egypt. SN Applied Sciences, 2(7), 1–14. https://doi.org/10.1007/s42452-020-3100-x

Séranne, M., & Anka, Z. (2005). South Atlantic continental margins of Africa: a comparison of the tectonic vs climate interplay on the evolution of equatorial west Africa and SW Africa margins. *Journal of African Earth Sciences*, *43*(1-3), 283-300.

Shedid SA (2018) A new technique for identification of flow units of shaly sandstone reservoirs. Journal of Petroleum Exploration Production Technology 8:495–504. https://doi.org/10.1007/s1320 2-017-0350-2

Shier, D. E. (2004). Well log normalization: methods and guidelines. *Petrophysics-The SPWLA Journal of Formation Evaluation and Reservoir Description*, *45*(03).

Stadtműller, M. & Jarzyna, J.A. (2023). Estimation of petrophysical parameters of carbonates based on well logs and laboratory measurements, a review. Energies, 16(10), (p4215).

Stollhofen, H. (1999). Karoo Synrift-Sedimentation und ihre tektonische Kontrolle am entstehenden Kontinentalrand Namibias. *Zeitschrift der deutschen geologischen Gesellschaft*, *149*, 519-632.

Utjavari, U. Hydrocarbon Potential of the Walvis Basin, Offshore Namibia. In *2018 AAPG International Conference and Exhibition*.

Wildman, M., Gallagher, K., Chew, D., & Carter, A. (2021). From sink to source: Using offshore thermochronometric data to extract onshore erosion signals in Namibia. *Basin Research*, *33*(2), 1580-1602.

Zhang, B., & Xu, J. (2016). Methods for the evaluation of water saturation considering TOC in shale reservoirs. *Journal of Natural Gas Science and Engineering*, *36*, 800-810.

Zhu, P.Y., You, L., Yuan, Q.T., Zhong, J., & Liu, A.Q. (2018). Mechanism and distribution of calcareous interbeds in songtao uplift and its periphery of Qiongdongnan Basin. Open Journal of Marine Science, 8(03). 370.

APPENDICES

APPENDIX 1: Ethical Clearance Certificate

UNAM
UNIVERSITY OF NAMIBIA

ETHICAL CLEARANCE CERTIFICATE

Ethical Clearance Reference Number: SOC/0006 **Date: 29 September 2022**

This Ethical Clearance Certificate is issued by the University of Namibia Ethics Committee (REC) in accordance with the University of Namibia's Research Ethics Policy and Guidelines. Ethical approval is given in respect of undertakings contained in the Research Project outlined below. This Certificate is issued on the recommendations of the ethical evaluation done by the ethics committee.

Title of Project: CHARACTERISATION OF THE RESERVOIR POTENTIAL OF THE H-T FIELD, OFFSHORE WALVIS BASIN, NAMIBIA

Principal researchers: Joel Ndangi Iyambo

Staff Number/ Student number: 200212125

Remarks: None

Centre for Research Services

Take note of the following:

1. Any significant changes in the conditions or undertakings outlined in the approved Proposal must be communicated to the ethics committee. An application to make amendments may be necessary.
2. Any breaches of ethical undertakings or practices that have an impact on ethical conduct of the research must be reported to the ethics committee
3. The Principal Researcher must report issues of ethical compliance to the ethics committee (through the Chairperson) at the end of the Project or as may be requested by the ethics committee
4. The ethics committee retains the right to:

i) Withdraw or amend this Ethical Clearance if any unethical practices (as outlined in the Research Ethics Policy) have been detected or suspected,

ii) Request for an ethical compliance report at any point during the course of the research.

The ethics committee wishes you the best in your research.

Dr Josefina T Hamutoko (Chairperson Decentralized Ethics Committee)

Prof. Davis Mumbengegwi (Head, Multidisciplinary Research)